POSIVA 97-13

Through-diffusion, permeability, channel-flow and *in situ* results for porosity and migration properties of rock samples by He-gas methods

Kari Hartikainen
Juhani Hartikainen
Oy Helium Gas Research HGR Ltd

Jussi Timonen
Department of Physics
University of Jyväskylä

December 1997

POSIVA OY
Mikonkatu 15 A, FIN-00100 HELSINKI, FINLAND
Phone (09) 2280 30 (nat.), (+358-9-) 2280 30 (int.)
Fax (09) 2280 3719 (nat.), (+358-9-) 2280 3719 (int.)

ISBN 951-652-038-3
ISSN 1239-3096

OY HELIUM GAS RESEARCH HGR LTD

SAATE **18.12.1997**

POSIVA OY
Aimo Hautojärvi
Mikonkatu 15 A
00100 HELSINKI

Tilauksiin 9656/96/LPN ja 9653/96/LPN viitaten ohessa raportin tarkastajien ja hyväksyjien allekirjoitukset.

Oy Helium Gas Research HGR Ltd

Kari Hartikainen
Toimitusjohtaja

Jyväskylän yliopisto

Jussi Timonen
professori

Posiva-raportti – Posiva report

Posiva Oy
Mikonkatu 15 A, FIN-00100 HELSINKI, FINLAND
Puh. (09) 2280 30 – Int. Tel. +358 9 2280 30

Raportin tunnus – Report code
POSIVA 97-13

Julkaisuaika – Date
December 1997

Tekijä(t) – Author(s)
Kari Hartikainen, Juhani Hartikainen,
Oy Helium Gas Research HGR Ltd
Jussi Timonen,
University of Jyväskylä

Toimeksiantaja(t) – Commissioned by
Posiva Oy

Nimeke – Title

THROUGH-DIFFUSION, PERMEABILITY, CHANNEL-FLOW AND *IN SITU* RESULTS FOR POROSITY AND MIGRATION PROPERTIES OF ROCK SAMPLES BY He-GAS METHODS

Tiivistelmä – Abstract

Rock samples from three candidate sites for nuclear waste repositories at Olkiluoto, Kivetty and Romuvaara were analysed by He-gas methods, and their porosities, diffusivities and permeabilities were determined.
The through-diffusion method was used to determine the porosities and effective diffusion coefficients of the short drill-core samples, and the permeability method to measure their permeability coefficients. The channel-flow method was used to determine the products of porosity and effective diffusion coefficient for the long drill-core samples. The matrix porosities and effective diffusion coefficients determined are for helium in samples saturated with nitrogen gas. The measured through-diffusion porosities varied between 0.03 and 2.20 %, and the effective diffusion coefficients of helium in samples saturated by nitrogen gas between 3.20×10^{-10} and 1.30×10^{-8} m^2/s. The measured permeability coefficients varied between 4.65×10^{-21} and 8.97×10^{-19} m^2. The products of porosity and effective diffusion coefficient measured by the channel-flow method varied between 4.0×10^{-16} and 2.7×10^{-13} m^2/s.
The results of the channel-flow measurements were in each case smaller than the corresponding results obtained from the through-diffusion measurements. There was a close correspondence between the effective diffusion coefficients and permeability coefficients. Three series of drill-core samples were measured by the helium-gas through-diffusion and permeability methods in order to determine the effect of sawing and sample length on the porosity and migration properties of rock samples. The measured porosities varied between 0.03 and 0.25 %, the effective diffusion coefficients of helium in samples saturated by nitrogen gas between 2.50×10^{-10} and 9.00×10^{-9} m^2/s and the permeability coefficients between 3.29×10^{-21} and 2.95×10^{-19} m^2.
The measured porosities, and diffusion and permeability coefficients indicate that sawing seems to have a very small effect on the measured rock characteristics in pure migmatitic mica gneiss samples. Correspondingly, it seems to have a minor effect in mica gneiss and granite samples. On the other hand, in granodiorite samples sawing seems to affect the characteristics. *In situ* measurements were repeated for two of the six drill holes in the TVO Research Tunnel at Olkiluoto, and the effect of bedrock rest humidity on the migration properties was analysed. Channel-flow measurements were also made on five long drill-core samples from these six drill holes, and through-diffusion measurements on six short pieces of these samples, in order to compare the results of all three methods. The measured porosities varied in the range from 0.04 to 0.15 %, the effective diffusion coefficients of helium in samples saturated by nitrogen gas from 4.50×10^{-11} to 2.00×10^{-9} m^2/s and their products from 1.80×10^{-14} to 3.00×10^{-12} m^2/s (through-diffusion), from 2.2×10^{-15} to 2.0×10^{-12} m^2/s (channel flow) and from 1.0×10^{-14} (8.0×10^{-16} measured in 1996) to 8.0×10^{-13} m^2/s (*in situ*).
The results determined show that the products of porosity and effective diffusion coefficient are on the average fairly similar for all methods. Different methods for same sections of drill holes produce results that appreciably differ only in few cases. The *in situ* results measured in 1995 and 1996 for drill hole VLJ-KR15 (depth 125-195 cm) differed by a factor 25. This deviation could not be explained. The above mentioned samples and holes were not exactly from the same sections, however, and there may also be some differences in the characteristics of the measured samples. The effect of bedrock rest humidity was observed to be negligible on the measured migration properties if the so-called mixture ratio, which describes the level of humidity of the outflowing gases in the measurements, was under 10 g/kg.

Avainsanat - Keywords
He-gas method, porosity, effective diffusion coefficient, permeability coefficient, bedrock rest humidity

ISBN
ISBN 951-652-038-3

ISSN
ISSN 1239-3096

Sivumäärä – Number of pages
43

Kieli – Language
English

Posiva-raportti – Posiva report

Posiva Oy
Mikonkatu 15 A, FIN-00100 HELSINKI, FINLAND
Puh. (09) 2280 30 – Int. Tel. +358 9 2280 30

Raportin tunnus – Report code
POSIVA 97-13

Julkaisuaika – Date
Joulukuu 1997

Tekijä(t) – Author(s)

Kari Hartikainen, Juhani Hartikainen,
Oy Helium Gas Research HGR Ltd
Jussi Timonen,
Jyväskylän yliopisto

Toimeksiantaja(t) – Commissioned by

Posiva Oy

Nimeke – Title

He-KAASUMENETELMILLÄ MÄÄRITETTYJÄ LÄPIDIFFUUSIO-, PERMEABILITEETTI-, KANAVA- JA *IN SITU* -MITTAUSTULOKSIA KIVINÄYTTEIDEN HUOKOISUUKSILLE JA KULKEUTUMISOMINAISUUKSILLE

Tiivistelmä – Abstract

He-kaasumenetelmällä mitattiin edustava määrä kivinäytteitä kolmesta mahdollisesta loppusijoituspaikkavaihtoehdosta Olkiluodosta, Kivetystä ja Romuvaarasta. Kivinäytteistä määritettiin niiden huokoisuudet sekä efektiiviset diffuusio- ja permeabiliteettikertoimet. Läpidiffuusiomittauksilla saadaan määritettyä näytteiden huokoisuus ja efektiivinen diffuusiokerroin. Permeabiliteettimittauksista saadaan vastaavasti selville näytteiden permeabiliteettikerroin. Kanavamittauksista saadaan selville huokoisuuden ja efektiivisen diffuusiokertoimen tulo tankokivinäytteille. Kaasufaasissa mitatut matriisihuokoisuudet ja efektiiviset diffuusiokertoimet määritettiin heliumin avulla näytteille, joiden huokoset olivat saturoituneet kaasumaisella typellä. Läpidiffuusiomenetelmällä määritetyt huokoisuudet vaihtelivat välillä 0.03 ja 2.20 % ja efektiiviset diffuusiokertoimet välillä 3.20×10^{-10} ja 1.30×10^{-8} m^2/s. Permeabiliteettikertoimet vaihtelivat vastaavasti välillä 4.65×10^{-21} ja 8.97×10^{-19} m^2. Kanavamittauksista määritetyt huokoisuuden ja efektiivisen diffuusiokertoimen tulot vaihtelivat välillä 4.0×10^{-16} ja 2.7×10^{-13} m^2/s. Tulokset osoittavat, että kanavamittaustulokset olivat säännöllisesti pienempiä kuin vastaavat läpidiffuusiomittaustulokset. Efektiivisten diffuusiokertoimien ja permeabiliteettikertoimien välillä näyttää olevan vahva riippuvuus. Kolme läpidiffuusionäytesarjaa tutkittiin sekä läpidiffuusio- että permeabiliteettimenetelmillä tarkoituksena selvittää kivinäytteiden sahauksen ja pituuden vaikutus niiden huokoisuus- ja kulkeutumisominaisuuksiin. Mitatut huokoisuudet vaihtelivat välillä 0.03 ja 0.25 %, heliumin avulla mitatut efektiiviset diffuusiokertoimet typpikaasulla saturoituneille näytteille välillä 2.50×10^{-10} ja 9.00×10^{-9} m^2/s ja permeabiliteettikertoimet välillä 3.29×10^{-21} ja 2.95×10^{-19} m^2. Mitatut huokoisuudet sekä efektiiviset diffuusio- että permeabiliteettikertoimet osoittivat, että sahauksella on erittäin pieni vaikutus kiven kulkeutumisominaisuuksiin puhtaille suuntautuneille kiillegneissinäytteille. Vastaavasti kiillegneissi- ja graniittinäytetapauksessa sahauksella havaittiin olevan pieni vaikutus kulkeutumisominaisuuksiin. Toisaalta granodioriittinäytteille sahaus aiheutti selvän muutoksen määritettyihin kulkeutumisominaisuuksiin. *In situ* -mittauksia toistettiin kahdessa (yhteensä kuudesta) kairanreiässä TVO:n louhintatunnelissa Olkiluodossa tarkoituksena analysoida peruskallion jäännöskosteuden vaikutusta kulkeutumisominaisuuksiin. Kanavamittauksia tehtiin myös viidelle tankokivinäytteelle ja läpidiffuusiomittauksia kuudelle lyhyelle läpidiffuusionäytteelle kaikkien kolmen menetelmän tulosten vertaamiseksi keskenään. Mitatut huokoisuudet vaihtelivat välillä 0.04 ja 0.15 %, efektiiviset diffuusiokertoimet välillä 4.50×10^{-11} ja 2.00×10^{-9} m^2/s ja niiden tulot välillä 1.80×10^{-14} ja 3.00×10^{-12} m^2/s (läpidiffuusiomenetelmä), välillä 2.2×10^{-15} ja 2.0×10^{-12} m^2/s (kanavamenetelmä) ja välillä 1.0×10^{-14} (8.0×10^{-16} mitattu 1996) ja 8.0×10^{-13} m^2/s (*in situ* -menetelmä). Määritetyt tulokset osoittavat, että huokoisuuksien ja efektiivisten diffuusiokertoimien tulot ovat keskimäärin hyvin samankaltaiset kaikille menetelmille. Eri menetelmillä saadut tulokset eroavat toisistaan vain muutamissa tapauksissa mitatuille kairanreikäsyvyyksille ja vastaavilta syvyyksiltä kairatuille läpidiffuusio- tai tankonäytteille. Vuosina 1995 ja 1996 kairanreiästä VLJ-KR15 (mittaussyvyys 125 - 195 cm) mitatut *in situ* -tulokset eroavat kuitenkin toisistaan tekijällä 25. Syytä tähän eroon ei pystytty selvittämään. Edellä mainitut kairanreikien mittaussyvyydet ja niitä vastaavat läpidiffuusio- ja tankokivinäytteet eivät tosin aivan tarkasti olleet samoista kohdista ja tämän lisäksi mitattujen näytteiden ominaisuuksissa saattaa olla eroavuuksia. Kallioperän jäännöskosteuden vaikutuksen kulkeutumisominaisuuksiin havaittiin lisäksi olevan merkityksetön, mikäli niin sanottu sekoitussuhde, joka kuvaa mittauksissa ulosvirtaavien kaasujen kosteustasoa, oli alle 10 g/kg.

Avainsanat - Keywords

He-kaasumenetelmä, huokoisuus, efektiivinen diffuusiokerroin, permeabiliteettikerroin, peruskallion jäännöskosteus

ISBN
ISBN 951-652-038-3

ISSN
ISSN 1239-3096

Sivumäärä – Number of pages
43

Kieli – Language
Englanti

TABLE OF CONTENTS

1 THROUGH-DIFFUSION, PERMEABILITY AND CHANNEL-FLOW MEASUREMENTS ON SAMPLES FROM POSIVA'S SITE INVESTIGATIONS IN OLKILUOTO, KIVETTY AND ROMUVAARA

1.1 Introduction

A collection of short and long drill-core samples from Posiva's site investigations at Olkiluoto, Kivetty and Romuvaara were measured and analysed. These series of measurements make it possible to complement the data which will be utilised to compare variations in the rock characteristics of the three candidate repository sites. For the same purpose, it is also useful to compare the results of through-diffusion and channel-flow methods. The main purpose of this study was both to test the correspondence between through-diffusion and channel-flow methods and to get more representative values for the bedrock characteristics of these sites. Finally, the permeability measurements were made to check the correspondence between the effective diffusion coefficients and permeability coefficients.

Five short and five long drill-core samples from both Olkiluoto (three types of rock) and Kivetty (two types of rock), and six short and six long drill-core samples (three types of rock) from Romuvaara were measured. In all, 32 samples were measured, consisting of 16 short and 16 long drill cores.

1.2 Measurements and samples

The through-diffusion and permeability measurements were made by using the standard methods described in detail in our previous reports (Väätäinen et al. 1993, Hartikainen et al. 1994a, Hartikainen et al. 1995a, Hartikainen et al. 1996a, Hartikainen et al. 1994b, Hartikainen et al. 1995b and Hartikainen et al. 1996b).

The channel-flow measurements were also made by the methods previously described. In addition the relative humidity, temperature and pressure of the gas were measured to ensure that the long drill-core samples were dry in these measurements.

The short drill-core samples were measured first by the through-diffusion and permeability methods. Before the measurements, all samples were kept under normal laboratory conditions without pre-drying. The diameters of the samples varied between 41.2 and 41.8 mm and their lengths between 19.1 and 22.5 mm. These thin samples were cut out from the ends of the long drill-core samples.

Secondly, the long drill-core samples were measured by the channel-flow method. Samples were dried by pure nitrogen gas in the measuring tube until the relative humidity was under 3% to make sure that the samples were dry enough. Typically, the drying time lasted for 10-15 hours. The flow rates that were used in the measurements varied between 1 and 70 ml/min. The aperture of the channel was 0.2 mm, its inner diameter was either 41.7 or 42.0 mm, and its length varied between 45.3 and 90.7 cm.

1.3 Results

The porosities measured by through-diffusion varied between 0.03 and 2.20 %, and the effective diffusion coefficients of helium in samples saturated by nitrogen gas between 3.20×10^{-10} and 1.30×10^{-8} m^2/s. The measured permeability coefficients varied between 4.65×10^{-21} and 8.97×10^{-19} m^2. Finally, the products of porosity and effective diffusion coefficent as measured by the channel flow method varied between 4.0×10^{-16} and 2.7×10^{-13} m^2/s. All the results are shown in Table 1. The measured break-through curves and the corresponding results of the model calculations are shown in Appendix A. Similarly, the results of channel-flow measurements are shown in Appendix B.

The correlation of the effective diffusion and permeability coefficients was found to be almost linear on the log-log scale. This confirmes our previous finding of the close relationship between these two quantities. This correlation is shown in Fig. 1. We also found that there were three short drill-core samples that were impermeable to gas (in both the through-diffusion and permeability measurements). These samples were OL-103 (mica gneiss, migmatitic), Ki-427 (porphyritic granodiorite, partially monzonite) and Ro-151 (granodiorite). They remained impermeable even under a pressure difference of about 200 kPa. Antero Lindberg (Geological Survey of Finland)

investigated these and some other samples, and his conclusions were the following.

Sample OL-103: nothing unusual, a rather dark sample; Ki-427: nothing unusual, a rather dark sample, one surface is slightly polished under sawing; Ro-151: a rather dark sample, one surface is slightly polished under sawing; OL-104: there is a volume (about 2×2×0.5 cm) of clay in one corner of the sample. In other words, the colouring of all three impermeable samples was rather dark. The possibility cannot therefore be ruled out that they have become (partly) saturated by some fluid used in drilling. The high porosity (2.2 %) of OL-104 is probably caused by the clay encloser in the sample.

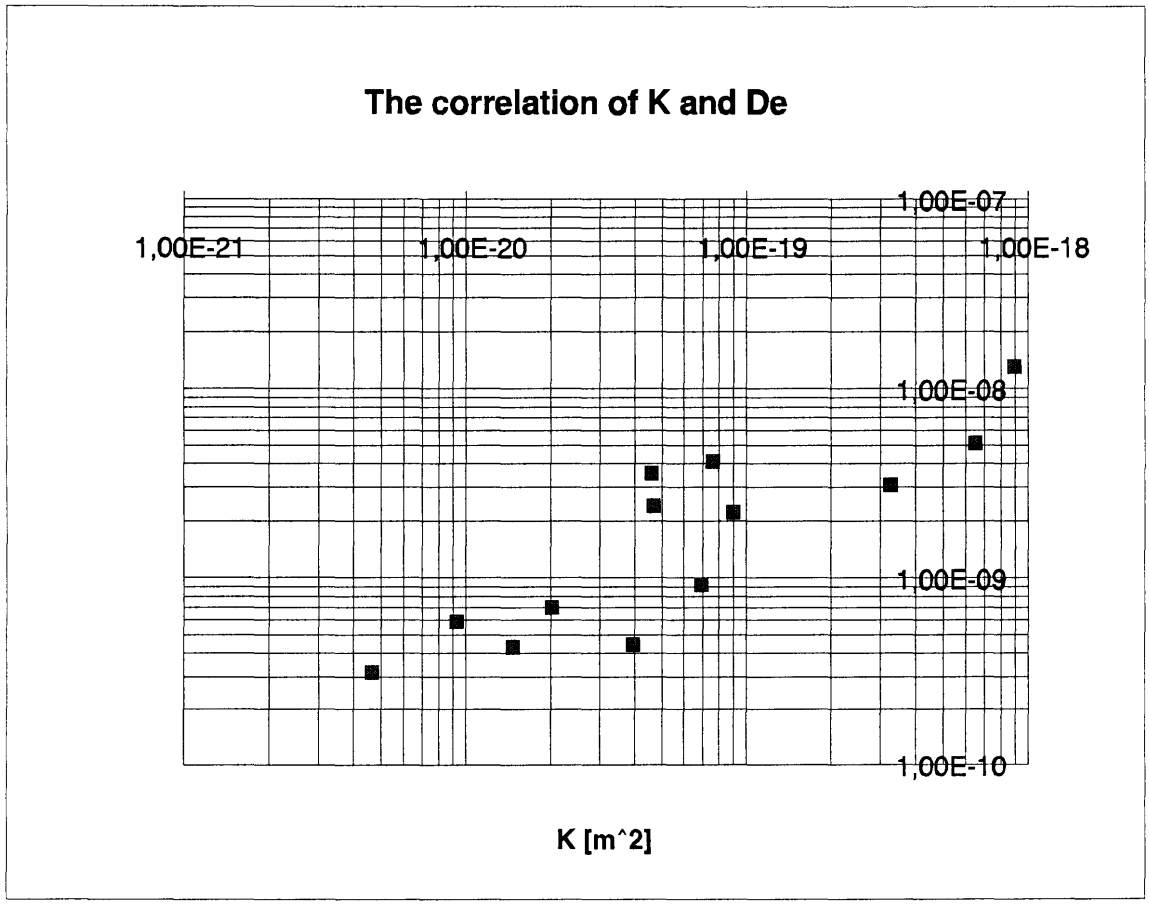

Figure 1. *Correlation of the effective diffusion and permeability coefficients.*

Table 1. Porosities, effective diffusion coefficients and permeability coefficients of the through-diffusion, permeability and channel-flow samples from Olkiluoto, Kivetty and Romuvaara. Diffusion coefficients are for helium in samples saturated by nitrogen gas ($D_e(He/N_2)$).

Sample	Rock type	Permeability K	Through-diffusion ε_p	D_e	$\varepsilon_p \times D_e$	Channel flow $\varepsilon_p \times D_e$
		[m^2]	[%]	[m^2/s]	[m^2/s]	[m^2/s]
OLKILUOTO						
OL-103	Mica gneiss (migmatitic)	-	-	-	-	6.0×10^{-14}
OL-104	Mica gneiss (migmatitic)	4.65×10^{-21}	2.2	3.20×10^{-10}	7.04×10^{-12}	2.5×10^{-13}
OL-206	Granite	6.47×10^{-19}	0.12	5.20×10^{-9}	6.24×10^{-12}	2.710^{-13}
OL-210	Tonalite	2.02×10^{-20}	0.28	7.00×10^{-10}	1.96×10^{-12}	2.7×10^{-13}
OL-211	Tonalite	1.47×10^{-20}	0.07	4.40×10^{-10}	3.08×10^{-13}	1.6×10^{-13}
KIVETTY						
Ki-419	Porphyritic granodiorite *	3.24×10^{-19}	0.03	3.10×10^{-9}	9.30×10^{-13}	2.2×10^{-13}
Ki-420	Porphyritic granodiorite *	6.93×10^{-20}	0.04	9.40×10^{-10}	3.76×10^{-13}	2.0×10^{-13}
Ki-427	Porphyritic granodiorite *	-	-	-	-	4.0×10^{-14}
* partially monzonite						
Ki-429	Porphyritic granite	3.94×10^{-20}	0.055	4.50×10^{-10}	2.48×10^{-13}	1.0×10^{-13}
Ki-434	Porphyritic granite	7.55×10^{-20}	0.11	4.10×10^{-9}	4.51×10^{-12}	2.1×10^{-15}
ROMUVAARA						
Ro-138	Mica gneiss *	9.17×10^{-21}	0.12	6.00×10^{-10}	7.20×10^{-13}	2.8×10^{-15}
Ro-139	Mica gneiss *	8.97×10^{-19}	0.2	1.30×10^{-8}	2.60×10^{-11}	1.05×10^{-15}
* migmatitic						
Ro-144	Leukotonalite (gneiss)	9.00×10^{-20}	0.11	2.20×10^{-9}	2.42×10^{-12}	4.0×10^{-16}
Ro-147	Leukotonalite (gneiss)	4.71×10^{-20}	0.17	2.40×10^{-9}	4.08×10^{-12}	2.8×10^{-15}
Ro-150	Granodiorite	4.57×10^{-20}	0.12	3.60×10^{-9}	4.32×10^{-12}	3.5×10^{-15}
Ro-151	Granodiorite	-	-	-	-	7.0×10^{-15}

It is evident that the channel-flow results (the products $\varepsilon_p \times D_e$) are in each case smaller than the corresponding results obtained from the through-diffusion measurements.

As in our previous studies, the previous results show that the biggest differences between the through-diffusion and channel-flow results are in the mica gneiss (micmatitic) and the leukotonalite samples from Romuvaara. We have previously

suggested that this discrepancy may have been caused by e.g. microcracks in these short drill-core samples. However, this explanation could now be ruled out. Both the through-diffusion and permeability results are mutually consistent for all short samples. If there were a microcrack in a thin sample, the permeability coefficient would indicate this much more clearly than the effective diffusion coefficient. It has also been suggested before that finite-size effects in the through-diffusion results might contribute to the observed difference in the results. These effects were now analysed, and it appeared that if the length of the through-diffusion samples was more than about 20 mm, there was no detectable finite-size effect in the through-diffusion measurements. A more detailed account of these results is given in Section 2 of this report.

The most probable reason therefore for the difference in the through-diffusion and channel-flow results is the direction of migration paths. In the through-diffusion measurements, these pathways are mainly in the axial direction and in the channel-flow measurements mainly in the radial direction. If the structure of the studied rock type is anisotropic, the measured results (migration properties) may vary as a function of the direction. If this is the explanation, anisotropy may play an important role in the migration behaviour. A more detailed analysis of this phenomenon is clearly needed.

It is also evident from the results in Table 2, in which the present results and also those of our previous studies of the three repository sites are shown, that there are often significant variations in the product $\varepsilon_p \times D_e$ even within a given rock type from one site.

Table 2. Porosities and effective diffusion coefficients for the channel-flow and through-diffusion samples from Olkiluoto, Kivetty and Romuvaara. Diffusion coefficients are for helium in samples saturated by nitrogen gas ($D_e(He/N_2)$).

Sample	Rock type		Through-diffusion ε_p [%]	Through-diffusion D_e [m^2/s]	Through-diffusion $\varepsilon_p \times D_e$ [m^2/s]	Channel flow $\varepsilon_p \times D_e$ [m^2/s]
OLKILUOTO						
OL-100	Mica gneiss (migmatitic)		0.018	1.05×10^{-10}	1.89×10^{-14}	1.00×10^{-15}
OL-101	Mica gneiss (migmatitic)		-	-	-	1.30×10^{-14}
OL-102	Mica gneiss (migmatitic)		0.075	2.3×10^{-10}	1.73×10^{-13}	7.00×10^{-16}
OL-103	Mica gneiss (migmatitic)		-	-	-	6.00×10^{-14}
OL-104	Mica gneiss (migmatitic)		2.2	3.20×10^{-10}	7.04×10^{-12}	2.50×10^{-13}
OL-206	Granite		0.12	5.20×10^{-9}	6.24×10^{-12}	2.70×10^{-13}
OL-207	Granite		0.11	4.60×10^{-9}	5.06×10^{-12}	3.00×10^{-14}
OL-208	Granite		0.09	6.55×10^{-9}	5.90×10^{-12}	2.00×10^{-14}
OL-209	Granite		-	-	-	8.00×10^{-14}
OL-210	Tonalite		0.28	7.00×10^{-10}	1.96×10^{-12}	2.70×10^{-13}
OL-211	Tonalite		0.07	4.40×10^{-10}	3.08×10^{-13}	1.60×10^{-13}
OL-212	Tonalite		-	-	-	1.00×10^{-13}
OL-213	Tonalite	(slice 1)	0.07	6.60×10^{-10}	4.62×10^{-13}	1.60×10^{-13}
		(slice 2)	0.09	2.80×10^{-10}	2.52×10^{-13}	
OL-214	Tonalite		-	-	-	1.00×10^{-14}
KIVETTY						
Ki-416	Porphyritic granodiorite *		0.085	7.80×10^{-9}	6.63×10^{-12}	3.00×10^{-13}
Ki-419	Porphyritic granodiorite *		0.03	3.10×10^{-9}	9.30×10^{-13}	2.20×10^{-13}
Ki-420	Porphyritic granodiorite *		0.04	9.40×10^{-10}	3.76×10^{-13}	2.00×10^{-13}
Ki-422	Porphyritic granodiorite *		0.0475	1.70×10^{-9}	8.08×10^{-13}	2.00×10^{-13}
Ki-425	Porphyritic granodiorite *		-	-	-	1.00×10^{-14}
Ki-427	Porphyritic granodiorite *		-	-	-	4.00×10^{-14}
* partially monzonite						
Ki-429	Porphyritic granite		0.055	4.50×10^{-10}	2.48×10^{-13}	1.00×10^{-13}
Ki-430	Porphyritic granite		-	-	-	1.00×10^{-14}
Ki-432	Porphyritic granite		0.0775	9.90×10^{-10}	7.67×10^{-13}	3.00×10^{-14}
Ki-433	Porphyritic granite		0.2	2.90×10^{-9}	5.80×10^{-12}	5.00×10^{-13}
Ki-434	Porphyritic granite		0.11	4.10×10^{-9}	4.51×10^{-12}	2.10×10^{-15}
ROMUVAARA						
Ro-136	Mica gneiss *		-	-	-	1.90×10^{-14}
Ro-137	Mica gneiss *	(slice 1)	0.15	9.85×10^{-9}	1.48×10^{-11}	2.50×10^{-16}
		(slice 2)	0.22	2.50×10^{-8}	5.50×10^{-11}	
Ro-138	Mica gneiss *		0.12	6.00×10^{-10}	7.20×10^{-13}	2.80×10^{-15}
Ro-139	Mica gneiss *		0.2	1.30×10^{-8}	2.60×10^{-11}	1.05×10^{-15}
Ro-141	Mica gneiss *		-	-	-	6.00×10^{-15}
* migmatitic						
Ro-143	Leukotonalite (gneiss)		-	-	-	1.00×10^{-14}
Ro-144	Leukotonalite (gneiss)		0.11	2.20×10^{-9}	2.42×10^{-12}	4.00×10^{-16}
Ro-147	Leukotonalite (gneiss)		0.17	2.40×10^{-9}	4.08×10^{-12}	2.80×10^{-15}
Ro-148	Leukotonalite (gneiss)		0.1	2.20×10^{-9}	2.20×10^{-12}	5.00×10^{-13}
Ro-149	Leukotonalite (gneiss)		0.23	2.15×10^{-9}	4.95×10^{-12}	9.20×10^{-13}
Ro-150	Granodiorite		0.12	3.60×10^{-9}	4.32×10^{-12}	3.50×10^{-15}
Ro-151	Granodiorite		-	-	-	7.00×10^{-15}
Ro-152	Granodiorite		0.055	1.13×10^{-9}	6.22×10^{-13}	1.20×10^{-13}
Ro-153	Granodiorite		-	-	-	1.00×10^{-13}
Ro-154	Granodiorite		0.1	3.00×10^{-9}	3.00×10^{-12}	2.00×10^{-12}

Slice 1 is from the upper part and slice 2 from the lower part of the drill-core sample.

1.4 Conclusions

We have shown here that the effective diffusion coefficients and permeability coefficients determined are well correlated. This indicates that these quantities are closely related, i.e. that the dominating migration pathways in diffusion and pressure induced flow are very similar.

The results from the channel-flow measurements of long drill-core samples were in each case smaller than the corresponding results for short drill-core samples obtained from through-diffusion measurements. The differences between through-diffusion and channel-flow results were particularly clear in the mica gneiss (migmatitic) and leukotonalite samples from Romuvaara. The most probable reason for this difference is the anisotropy of rock such that migration properties may strongly depend on the direction of relevant paths. A more detailed analysis of this interesting phenomenon is clearly needed. Furthermore, the results show that in many cases there are significant variations in the product of porosity and diffusion coefficient even within a given rock type from one site.

It is also worth noting that there were three short drill-core samples that were impermeable to gas in both the through-diffusion and permeability measurements). They were impermeable even under a pressure difference of about 200 kPa. This may indicate that they have become (partly) saturated by some fluid possibly during the drilling. It is therefore important that more attention is paid to careful handling of samples during drilling in the future.

2 THE EFFECT OF SAWING AND SAMPLE LENGTH ON POROSITY AND MIGRATION PROPERTIES OF ROCK SAMPLES

2.1 Introduction

The effects of sawing and sample length of rock samples have been unknown or at least inadequately studied as far as its effect on porosities, effective diffusion coefficients and permeability coefficients is concerned. Sawing may however cause some disturbances close to the cutting surface. The main goal of this study was to investigate these effects on rock samples by studying the changes in porosities, effective diffusion coefficients and permeability coefficients for varying sample length.

It would not have been possible in practice to carry out this kind of research until the introduction of the He-gas method, because traditional liquid phase measurements would have been too time consuming.

2.2 Samples

Measurements were made on three series of cylindrical disk (drill-core) samples with a diameter of 41.7 mm. These samples were cored in connection with Posiva's site investigations at Romuvaara. The analysed samples were denoted by Ro-1411, Ro-1412 and Ro-1521. The rock type of Ro-1411 was migmatitic mica gneiss, at Ro-1412 both mica gneiss and granite, and at Ro-1521 granodiorite. For each series the original sample (e.g. Ro-1411a) was first measured and then cut into two halves (e.g. Ro-1411b and Ro-1411c). After measuring these two halves both Ro-1411b and Ro-1411c were further cut into two halves which were denoted by Ro-1411d, Ro-1411e, and by Ro-1411f, Ro-1411g, correspondingly. All sample series were handled and denoted in a similar way. The thicknesses and notations of all series are shown in Fig. 2.

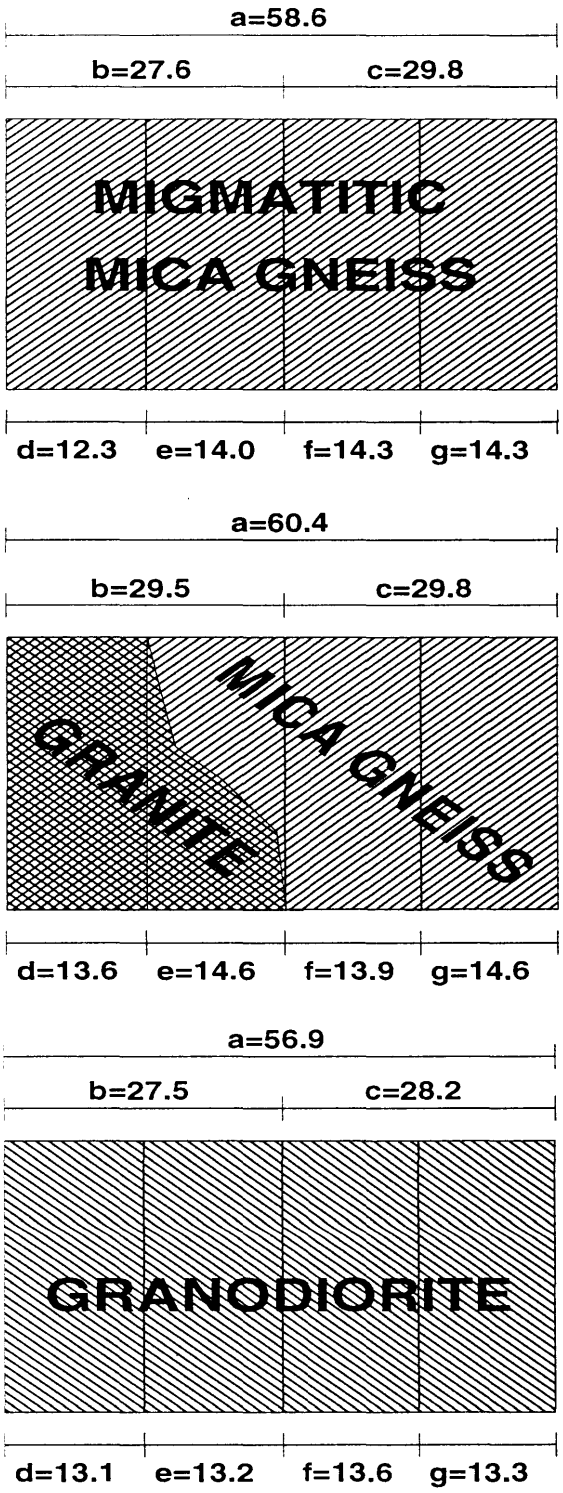

ROMUVAARA Ro-1

SAMPLE Ro-1411

ROMUVAARA Ro-1

SAMPLE Ro-1412

ROMUVAARA Ro-1

SAMPLE Ro-1521

Figure 2. The thicknesses (mm) and notations of the samples in all three series.

2.3 Measurements

The whole break-through curves and permeability data with several pressure differences of the 21 samples were measured, and the results were analysed by the mathematical models introduced in our previous reports. As a result from the fits, matrix porosities, effective diffusion coefficients of helium in samples saturated by nitrogen gas, and permeability coefficients in the gas phase were determined.

Before the measurements, all samples were kept under normal laboratory conditions without pre-drying.

2.4 Results

The observed porosities varied between 0.03 and 0.25 %, the effective diffusion coefficients $D_e(He/N_2)$ between 2.50×10^{-10} and 9.00×10^{-9} m^2/s and permeability coefficients between 3.29×10^{-21} and 2.95×10^{-19} m^2. In Table 3 we give the lengths, rock types, porosities, and effective diffusion coefficients of helium in samples saturated by nitrogen gas and permeability coefficients for all samples. The measured through-diffusion curves and the corresponding results of model calculations are shown in Appendix C.

It is evident from the results shown in Table 3 that for the sample series Ro-1411 there are no essential differences in the results before and after sawing. Also, sawing has a minor effect on the sample series Ro-1412. The original sample of this sample series was composed of two types of rock: mica gneiss and granite. These two halves behaved in a similar way in that only a minor effect of sawing could be detected. In the third sample series Ro-1521, there was a clear effect after the second cuts. After the first cut the results were rather similar. The second shortening from about 28 mm to about 13 mm indicates some effects of sawing on migration properties and porosities. Because of sawing, the samples seem to become a bit tighter, i.e. there may be a surface effect. These samples (granodiorite) consist of granules with a diameter of about 1 mm. Sawing dust may penetrate into the grain boundaries between these granules with the

result that samples (the cutting surfaces) become tighter. Other effects are also possible.

Table 3. *Lengths, rock types, porosities, effective diffusion coefficients and permeability coefficients of all samples measured. The diffusion coefficients are for helium in samples saturated by nitrogen gas.*

Sample	**Rock type**	**Length** [mm]	**Porosity** [%]	**D_e (He/N_2)** [m^2/s]	**K** [m^2]
Ro-1411a	Migmatitic miga gneiss	58.6	0.20	8.80×10^{-9}	2.02×10^{-19}
Ro-1411b	Migmatitic miga gneiss	27.6	0.15	8.20×10^{-9}	2.32×10^{-19}
Ro-1411c	Migmatitic miga gneiss	29.8	0.15	8.50×10^{-9}	2.95×10^{-19}
Ro-1411d	Migmatitic miga gneiss	12.3	0.21	9.00×10^{-9}	1.96×10^{-19}
Ro-1411e	Migmatitic miga gneiss	14.0	0.19	9.00×10^{-9}	2.06×10^{-19}
Ro-1411f	Migmatitic miga gneiss	14.3	0.20	8.50×10^{-9}	1.78×10^{-19}
Ro-1411g	Migmatitic miga gneiss	14.3	0.20	8.80×10^{-9}	2.10×10^{-19}
Ro-1412a	Migmatitic miga gneiss	60.4	0.25	6.10×10^{-9}	1.26×10^{-19}
Ro-1412b	Granite	29.5	0.10	3.50×10^{-9}	1.39×10^{-19}
Ro-1412c	Miga gneiss	29.8	0.11	4.60×10^{-9}	1.88×10^{-19}
Ro-1412d	Granite	13.6	0.10	3.10×10^{-9}	8.46×10^{-20}
Ro-1412e	Granite	14.6	0.20	6.10×10^{-9}	1.20×10^{-19}
Ro-1412f	Miga gneiss	13.9	0.14	5.40×10^{-9}	1.12×10^{-19}
Ro-1412g	Miga gneiss	14.6	0.20	5.60×10^{-9}	1.19×10^{-19}
Ro-1521a	Granodiorite	56.9	0.22	1.20×10^{-9}	1.19×10^{-20}
Ro-1521b	Granodiorite	27.5	0.15	1.65×10^{-9}	1.50×10^{-20}
Ro-1521c	Granodiorite	28.2	0.18	1.30×10^{-9}	6.99×10^{-21}
Ro-1521d	Granodiorite	13.1	0.03	3.40×10^{-10}	5.46×10^{-21}
Ro-1521e	Granodiorite	13.2	0.035	5.80×10^{-10}	3.29×10^{-21}
Ro-1521f	Granodiorite	13.6	0.03	3.95×10^{-10}	8.73×10^{-21}
Ro-1521g	Granodiorite	13.3	0.035	2.50×10^{-10}	3.52×10^{-21}

When the studied sample series are compared, it can be seen that the values of the effective diffusion coefficients and permeability coefficients are smallest in the granodiorite samples. The porosity values are rather consistent in all series, except for the samples shorter than 15 mm in the case of granodiorite.

2.5 Conclusions

It is evident that in some rock types (e.g. granodiorite) sawing may affect the porosity and migration properties of the sample. In this study, the effect was most clearly observed in the granodiorite samples of about 13 mm long. Values measured for these short samples were clearly smaller than those for the longer samples.

As the sawing techniques used were not analysed here, a more systematic study of the effects of sawing on the porosity and migration properties of rock samples is needed.

3 MIGRATION PROPERTIES OF ROCK WITH He-GAS THROUGH-DIFFUSION, CHANNEL-FLOW AND *IN SITU* METHODS

3.1 Introduction

The effect of bedrock humidity on the migration properties as measured by the *in situ* method has not been evaluate before. High humidity is supposed to slow down the matrix diffusion because the water in the system should behave like a trap in He-gas measurements. This effect is however not taken into account in analysing the measured break-through curves. The first main goal of this study was to investigate the effect of humidity by studying the changes in the products of porosity and effective diffusion coefficient as a function of the humidity (mixture ratio) of the outflowing gas.

The second main goal of this study was to compare the results (the above mentioned products) determined by the *in situ*, channel-flow and through-diffusion methods, and thirdly to find out the possible effect of bedrock stress on migration properties. Yet another important issue was to accumulate more data and thereby to improve the statistics of the variations in the migration characteristics of bedrock at relevant sites.

3.2 Samples

In situ measurements were made on specified sections of two drill holes whose diameter was 56 mm. These holes (cored 1995, at a depth of about 100 m below the ground at Olkiluoto), and their locations in the experimental tunnel, are reported in our earlier report (Hartikainen et al. 1996b). Channel-flow measurements were made in laboratory for five long drill-core samples from the same sections of these drill holes. Through-diffusion measurements were made for six short samples cut from the ends of the long drill cores. The diameter of the channel-flow and through-diffusion samples was about 45.1 mm. The lengths of the channel-flow samples were from 0.50 to 0.75 m, and of the through-diffusion samples from 14.7 to 30.6 mm. The rock type in the holes measured and of the drill-core samples was tonalite. The results of the previous drill hole and drill-core measurements are given in our earlier reports.

3.3 Channel-flow and through-diffusion measurements

Channel-flow and through-diffusion measurements were made by using the standard techniques reported earlier. However, in this case the relative humidity, pressure and temperature of flowing gases were also measured in the channel-flow measurements. Using these quantities it was possible to calculate the mixture ratio of water vapour that the outflowing gases contained.

3.4 *In situ* measurements

A specially designed *in situ* equipment was used to measure the drill holes. The same equipment was also used to dry the sections measured from the holes. The basic measuring technique has been reported earlier. The same quantities were measured as in the channel flow measurements.

3.4.1 The effect of bedrock rest humidity

The *in situ* device was first calibrated by using several different flow rates of pure nitrogen gas. The device was put into a stainless steel tube and, for varying flow rates, the relative humidity, pressure and temperature of the nitrogen gas were measured. Using these quantities, it is possible to calculate the mixture ratio x [g/kg] (Eq. 1) for water vapour that the outflowing nitrogen contained (VAISALA 1996). We find that

$$x = 621{,}98 \cdot RH \cdot \frac{P_{ws}}{(100 \cdot p - RH \cdot P_{ws})} \quad , \qquad 1$$

where RH is the relative humidity [%], p the pressure of the system [mbar] and $\mathbf{P}_{ws}$ the partial pressure of water vapor [mbar] given (VAISALA 1996) by

$$P_{ws} = A \cdot 10^{\left(\frac{m \cdot T}{T + T_n}\right)} \quad . \qquad 2$$

Here A (=6.1078), m (=7.5000) and T_n (=237.3) are constants applicable in the

temperature (*T*) range -40 ... +50°C. The general conditions of the tunnel air were such that the relative humidity was 94.9 %, the pressure 1013 mbar and the temperature 10.1°C.

The measured calibration results and calculated mixture ratios are shown in Table 4. The mixture ratio as a function of flow rate is also shown in Fig. 3.

Table 4. *The results measured and mixture ratios determined for different flow rates in the stainless-tube calibration measurements.*

Flow rate [ml/min]	***T*** [°C]	***RH*** [%]	***p*** [mbar]	P_{ws} [mbar]	***x*** [g/kg]
35.53	10.1	5.7	383.6	12.3614	1.1446
31.03	10.2	8.3	517.4	12.4445	1.2441
25.27	10.1	12.0	646.9	12.3614	1.4295
19.29	10.1	15.6	753.9	12.3614	1.5950
13.61	10.4	20.4	840.3	12.6119	1.9102
7.69	10.2	23.0	919.2	12.4445	1.9428

The stabilisation time used at all flow rates was 20 min. From the Table 4 it is easy to deduce how the relative humidity depends on the flow rate. Due to this dependence, the mixture ratio must be used to measure the humidity of the gas. Furthermore, the mixture ratio is also a function of flow rate. Even though we used nitrogen from a gas bottle, there was some water vapour in the measuring system. A leak in the measuring system would explain the presence of water, but such a leak was not found. The mixture ratio measured as a function of flow rate is shown in Fig. 3.

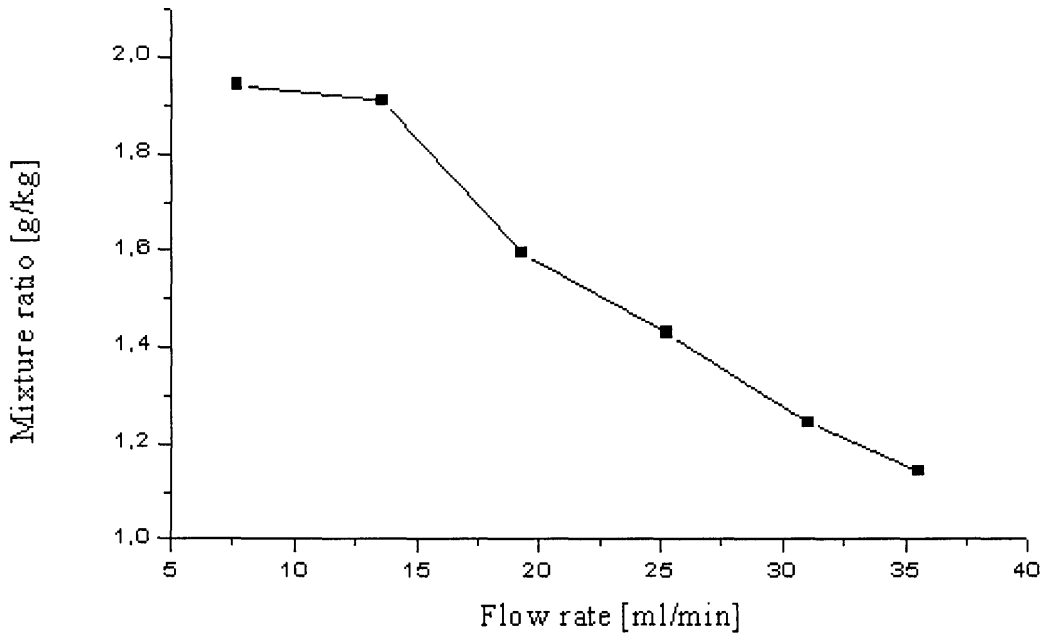

Figure 3. *The mixture ratio as a function of flow rate.*

After the calibration measurements, three sections from two drill holes were measured by using the same but also different flow rates. The drill holes were dryed by using pressurised pure nitrogen gas before each measurement. The typical drying time was about twelve hours, and a typical example of the measured results for two different values of relative humidity are shown in Fig. 4 (hole VLJ-KR15, depth 125-195 cm). The shapes of curves shown in Fig. 4 are very similar. Each section was measured at several values of relative humidity. The only quantity which seemed to change in the curves measured was the height of their maxima. However, these changes were small and their influence on the parameters determined was so small that it was neglected. The relative humidity varied from 40.6 to 75.9 %, the corresponding mixture ratio from 3.8010 to 6.9732 g/kg, and the flow rate used was 13.5 ml/min in these measurements.

Comparing these mixture ratios with those shown in Fig. 3, we find that the measured section from hole VLJ-KR15 contained some water (the mixture ratio determined for the flow rate of 13.5 ml/min was 1.915 g/kg in the calibration measurements).

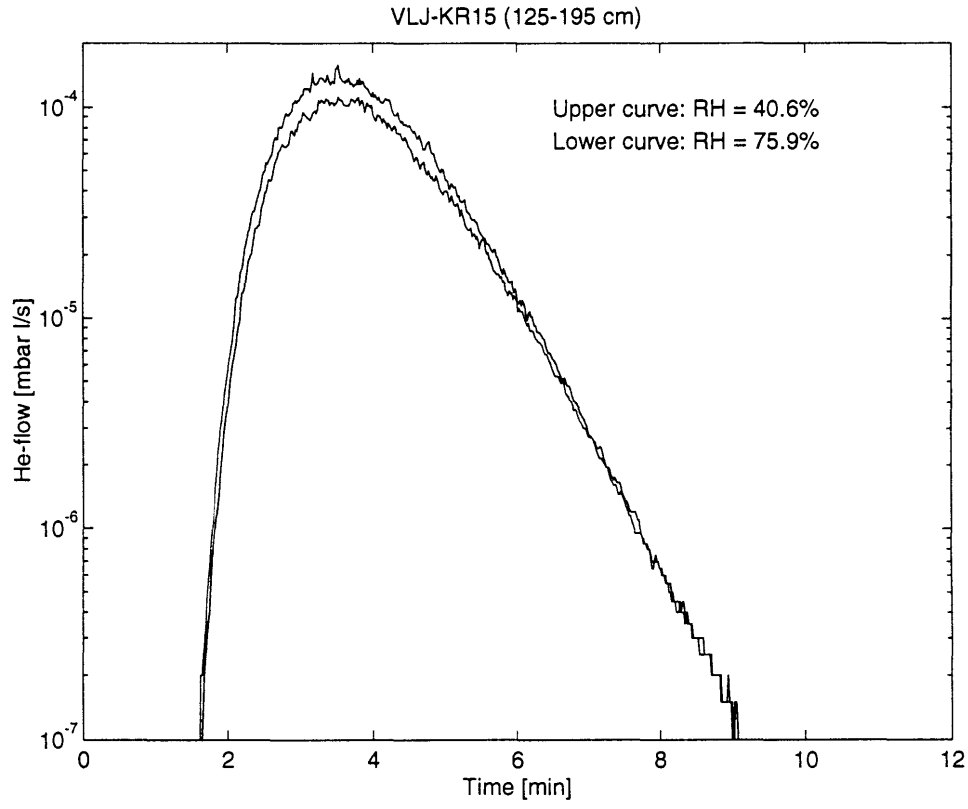

Figure 4. *Break-through curves measured by the in situ method on hole VLJ-KR15 (depth 125-195 cm) at a flow rate of 13.5 ml/min and for two relative humidities. The upper curve is for 40.6 % and the lower curve for 75.9 % relative humidity.*

On the basis of these and other measurements (the highest relative humidity measured was 85.6 %) we estimate that even a relatively high humidity of about 90 % (mixture ratios under about 10 g/kg) gives reasonable results in the *in situ* measurements.

3.5 Comparison of through-diffusion, channel-flow and *in situ* results

The second main goal of this study was to compare the results determined (products $e_p \times D_e$) by the *in situ*, channel-flow and through-diffusion methods, and also to analyse the possible effects of bedrock stress on migration properties. Another important issue was to accumulate more data for improving the statistics of the migration characteristics of bedrock at the relevant sites.

The long drill-core samples were dryed by nitrogen gas before the measurements. The typical drying time was about two hours. The short drill cores were kept in laboratory conditions before the measurements.

Flow rates in the *in situ* measurements were in the range 2 ml/min < Q < 33 ml/min. Only one drill hole (VLJ-KR15, depth 125-195 cm) was measured in this study to complement the results measured already before (Hartikainen et al. 1996a).

Flow rates in the channel-flow measurements were in the range 1 ml/min < Q < 75 ml/min. Channel-flow measurements were made on the samples taken from the sections measured in the *in situ* measurements. The drill-core sample taken from hole VLJ-KR16 (depth 175-245 cm) has also been measured earlier (Hartikainen et al. 1996a), and the result of this measurement is shown in Table 5.

For comparison, six thin (short) drill-core samples cut from the ends of the long drill-core samples were measured by the through-diffusion method.

All results measured are shown in Table 5. The *in situ* results from our previous report (Hartikainen et al. 1996a) are shown together with those for hole VLJ-KR15 (depth 125-195 cm) which were measured now. The channel-flow result for drill core VLJ-KR16 is also from our earlier report. All the other results are from this study. The measured through-diffusion, channel-flow and *in situ* curves, and the corresponding results of the model calculations, are shown in Appendices D, E and F.

For hole VLJ-KR15 (depth 125-195, measured 1996) the product $\varepsilon_p \times D_e$ (He/N_2) as found from the *in situ* measurement is 8.0×10^{-16} m^2/s. A similar measurement made in 1995 gave 2.0×10^{-14} m^2/s. Both the measured and fitted break-through curves are shown in Fig. 5. Measuring times were not equal because it was not possible to detect matrix diffusion for higher flow rates in 1996. The two results differ by a factor 25. This difference may be caused by bedrock humidity near the hole surface that has been different in the two measurements. However, measurements were made in a very similar way in both cases. In 1995 the humidity of the outflowing gases was not monitored, while now it was 80.4 % (mixture ratio 7.7 g/kg).

Table 5. *Products $\varepsilon_p \times D_e$ (He/N_2) from the in situ measurements at Olkiluoto, and from both the channel-flow and through-diffusion measurements on samples from the related drill cores.*

Drill hole	**Distance from the surface** [cm]	***In situ*** **$\varepsilon_p \times D_e$ (He/N_2)** [m^2/s]	**Channel flow** **$\varepsilon_p \times D_e$ (He/N_2)** [m^2/s]	**Through-diffusion** **$\varepsilon_p \times D_e$ (He/N_2)** [m^2/s]	
OLKILUOTO					
VLJ-KR11	122-192	1.0×10^{-14}	9.0×10^{-15}	1.17×10^{-13}	
VLJ-KR12	103-173	2.5×10^{-14}	2.2×10^{-14}	1.80×10^{-14}	
VLJ-KR14	175-245	9.0×10^{-14}	2.7×10^{-14}	8.10×10^{-14}	
VLJ-KR15A	18-88	1.3×10^{-13}	2.2×10^{-15}	3.00×10^{-12}	*
VLJ-KR15B	125-195	2.0×10^{-14}	6.0×10^{-15}	9.84×10^{-14}	
		8.0×10^{-16}	(measured in 1996)		
VLJ-KR16	175-245	8.0×10^{-13}	2.0×10^{-12}	4.00×10^{-14}	

* An obvious microcrack or microcracks through the thin sample.

Note: Distances from the surface are for the *in situ* measurements. Samples in the channel-flow and through-diffusion measurements were essentially from those sections used in the *in situ* measurements.

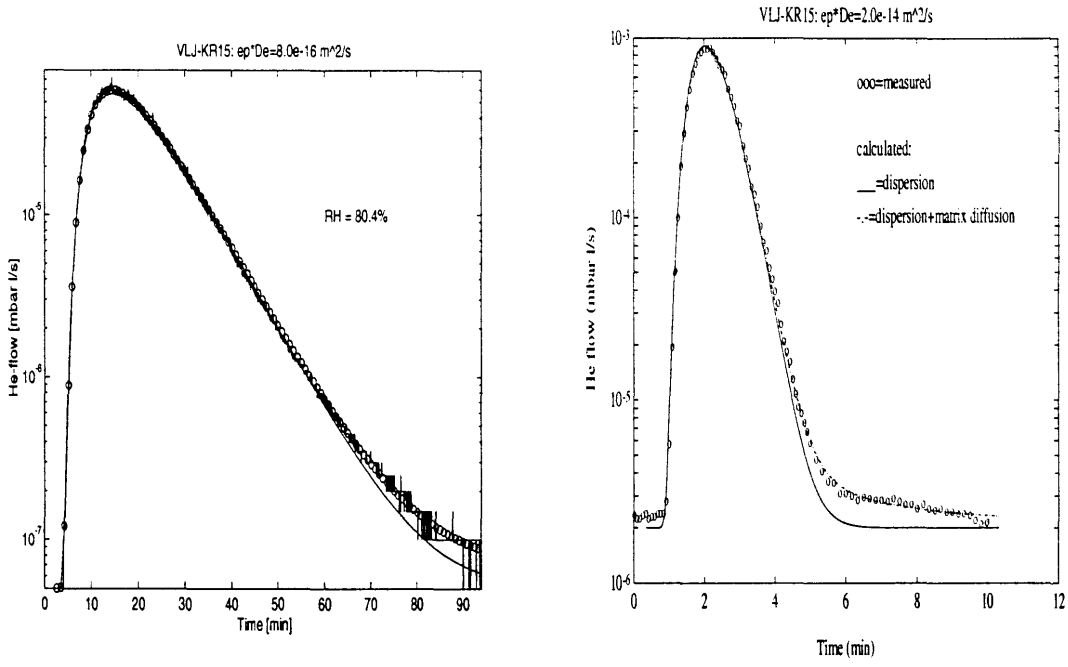

Figure 5. *Measured and fitted break-through curves for the in situ measurement done in 1996 (left) and in 1995 (right) on hole VLJ-KR15 (depth 125-195 cm). The effective diffusion coefficient is given for helium in samples saturated by nitrogen gas.*

In the case of VLJ-KR15 (depth 18-88 cm) the through-diffusion sample obviously contains a microcrack or microcracks, and the results obtained are not comparable with those of the other methods. We also find from the results shown in Table 4 that the channel-flow and *in situ* results are very similar apart from those for VLJ-KR15A. In comparing the channel-flow and through-diffusion results, agreement is rather good apart from mainly the results for VLJ-KR16. The *in situ* and through-diffusion results are also in good agreement generally, in this case a bigger difference was found between the present and 1996 results for VLJ-KR15B. There does not seem to be any systematic origin for the bigger differences. It is also expected that there are bigger variations in the through-diffusion results because of local variations in rock.

3.6 Conclusions

It seems that in the *in situ* measurements drying of the section of the drill hole to be measured is not critical. Typically the drying time of twelve hours was found to be enough. The effect of bedrock humidity was observed to be small on the migration properties if the so-called mixture ratio was under 10 g/kg.

By comparing the *in situ*, channel-flow and through-diffusion measurements, results are, apart from few exception, in fairly good agreement. No systematic effect of stress inside the bedrock was detected. However, it may well be so small at a depth of 100 m at Olkiluoto that it cannot be detected with the present accuracy. Measurements were also made relatively close to the tunnel surface so that stress relaxation may be appreciable.

In situ results from the measurements in 1995 and 1996 on hole VLJ-KR15 (depth 125-195 cm) differ by a factor 25. No clear explanation for this difference was found.

REFERENCES

Hartikainen, J., Hartikainen, K., Pietarila, H. & Timonen, J. 1995a. Permeability and diffusivity measurements with the He-gas method of disturbed zone in rock samples cored from the full-scale experimental deposition holes in the TVO Research Tunnel. Helsinki. Nuclear Waste Commission of Finnish Power Companies. Report YJT-95-16. 20 p. + app. 18 p. ISSN-0359-548X.

Hartikainen, J., Hartikainen, K., Hautojärvi, A., Kuoppamäki, K. & Timonen, J. 1996a. Helium gas methods for rock characteristics and matrix diffusion. Helsinki. Posiva Oy. Report POSIVA-96-22. 58 p. + app. 13 p. ISBN 951-652-021-9.

Hartikainen, K., Väätäinen, K., Hautojärvi, A. & Timonen, J. 1994a. Further development and studies of gas methods in matrix diffusion. In: Barkatt, A. & Van Konynenburg, R. (eds). Scientific Basis for Nuclear Waste Management XVII. Boston, USA. 1994. MRS Vol. 333. Pittsburgh. MRS. Pp. 821-826.

Hartikainen, K., Timonen, J., Väätäinen, K., Pietarila, H. & Hautojärvi, A. 1994b. Studies of matrix diffusion in gas phase (in Finnish). Helsinki. Nuclear Waste Commission of Finnish Power Companies. Report YJT-94-07. 27 p. + app. 2 p. ISSN-0359-548X.

Hartikainen, K., Hautojärvi, A., Pietarila, H. & Timonen, J. 1995b. Diffusion measurements on crystalline rock matrix. In: Murakami, T. & Ewing, R. (eds). Scientific Basis for Nuclear Waste Management XVIII. Boston, USA. 1995. MRS Vol. 353. Pittsburgh. MRS. Pp. 435-440.

Hartikainen, K., Pietarila, H., Rasilainen, K., Nordman, H., Ruskeeniemi, T., Hölttä, P., Siitari-Kauppi M. & Timonen, J. 1996b. Characterization of the altered zone around a fracture in Palmottu natural analogue. In: Murphy, W. & Knecht, D. (eds). Scientific Basis for Nuclear Waste Management XIX. Boston, USA. 1996. MRS Vol. 412. Pittsburgh. MRS. Pp. 839-846.

VAISALA 1996. HMP230-SARJAN LÄHETTIMET Käyttöohje, HMP230-U152fi-1.3, s. Liite 6: Laskentakaavat (in Finnish), 10. tammikuuta 1996.

Väätäinen, K., Timonen, J. & Hautojärvi, A. 1993. Development of a gas method for migration studies in fractured and porous media. In: Interrante, C. & Pabalan, R. (eds). Scientific basis for nuclear waste management XVI. Boston, USA. 1993. MRS Vol. 294. Pittsburgh. MRS. Pp. 851-856.

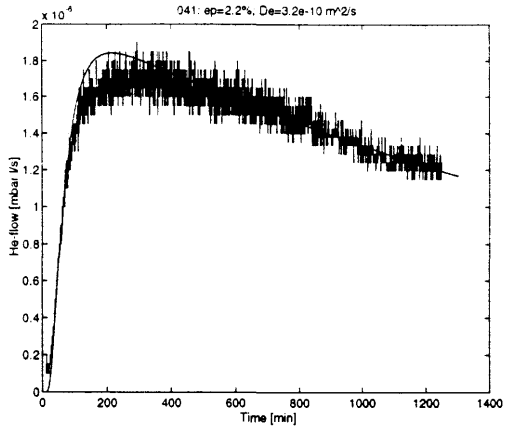

Figure 1. *Measured and fitted break-through curves for the sample OL-104.*

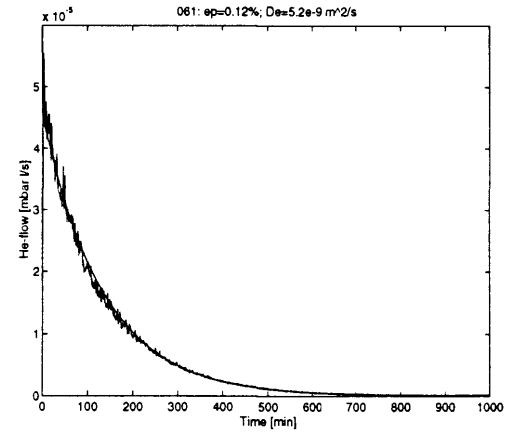

Figure 2. *Measured and fitted break-through curves for the sample OL-206.*

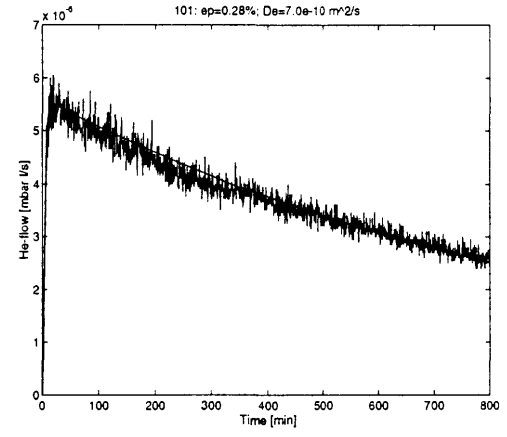

Figure 3. *Measured and fitted break-through curves for the sample OL-210.*

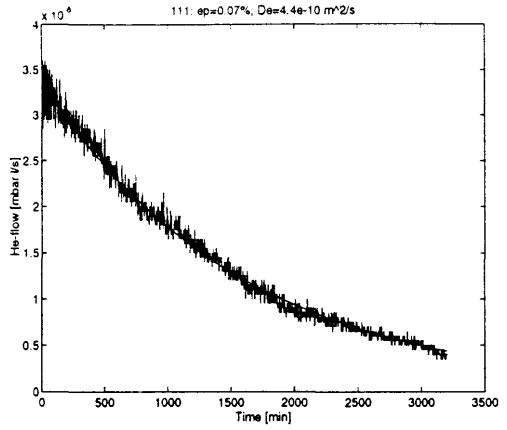

Figure 4. *Measured and fitted break-through curves for the sample OL-211.*

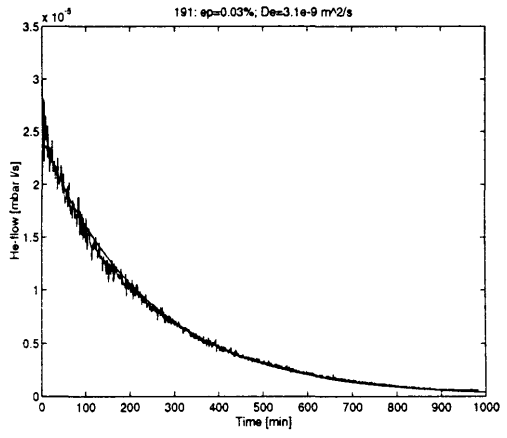

Figure 5. *Measured and fitted break-through curves for the sample Ki-419.*

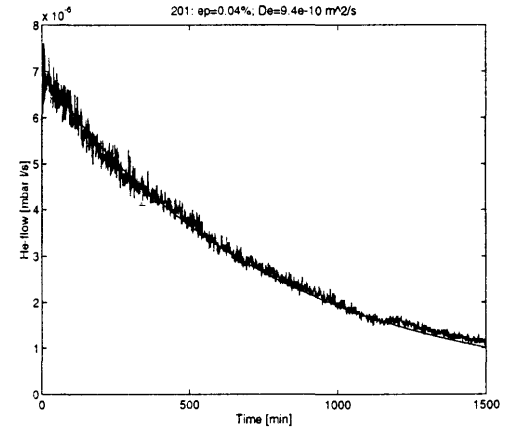

Figure 6. *Measured and fitted break-through curves for the sample Ki-420.*

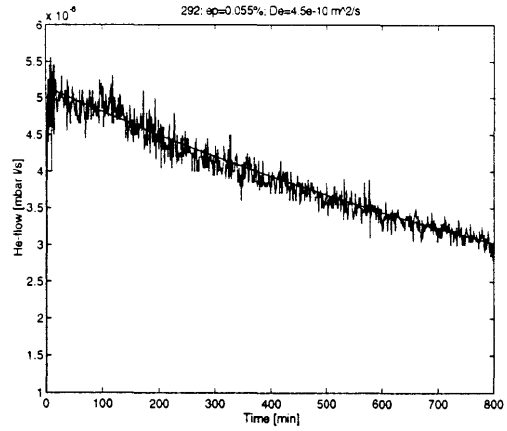

Figure 7. Measured and fitted break-through curves for the sample Ki-429.

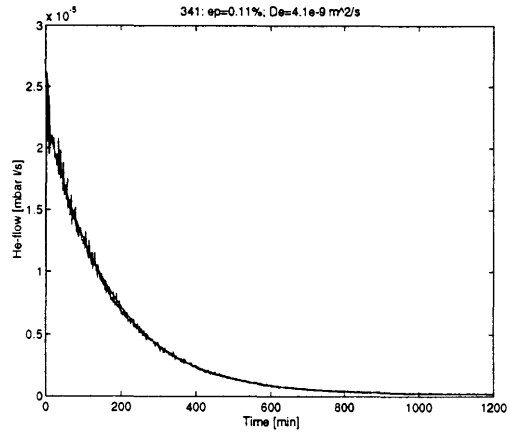

Figure 8. Measured and fitted break-through curves for the sample Ki-434.

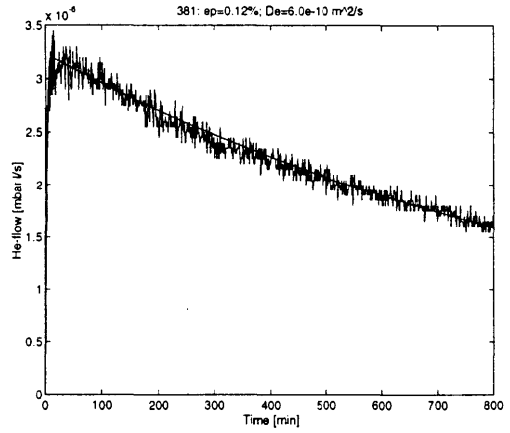

Figure 9. Measured and fitted break-through curves for the sample Ro-138.

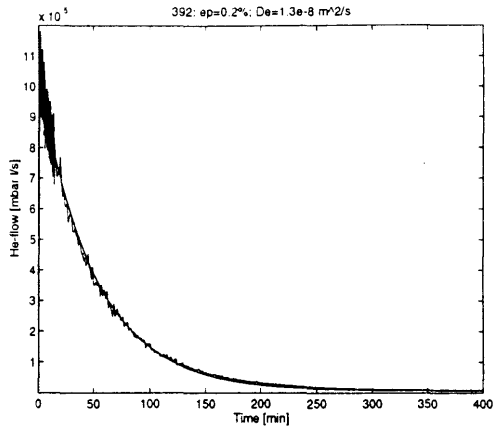

Figure 10. Measured and fitted break-through curves for the sample Ro-139.

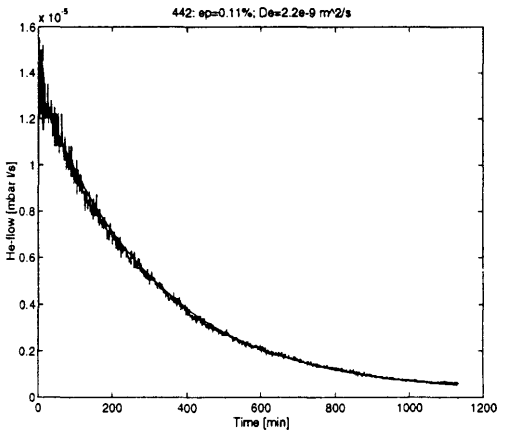

Figure 11. Measured and fitted break-through curves for the sample Ro-144.

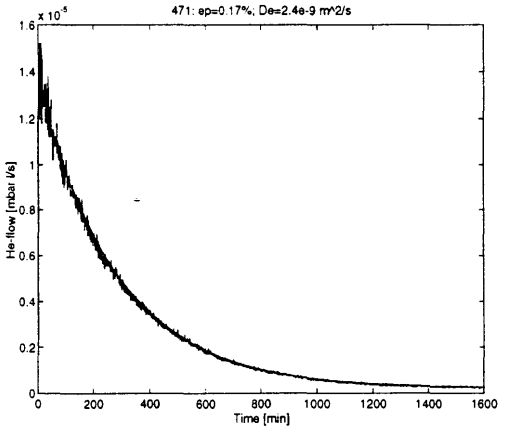

Figure 12. Measured and fitted break-through curves for the sample Ro-147.

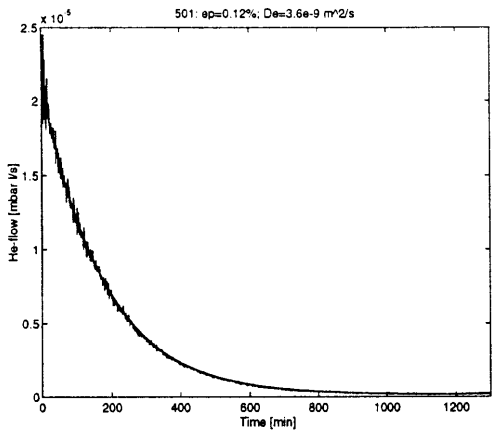

Figure 13. *Measured and fitted break-through curves for the sample Ro-150.*

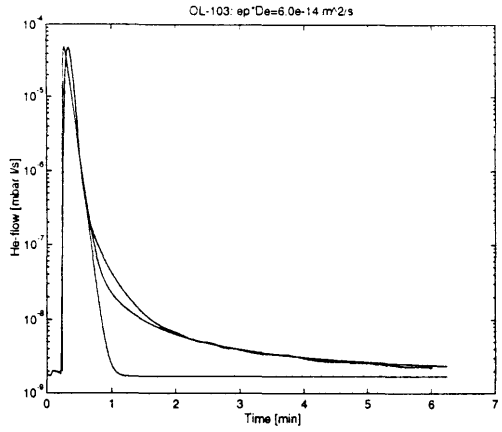

Figure 1. *Measured and fitted break-through curves for channel flow measurement on sample OL-103.*

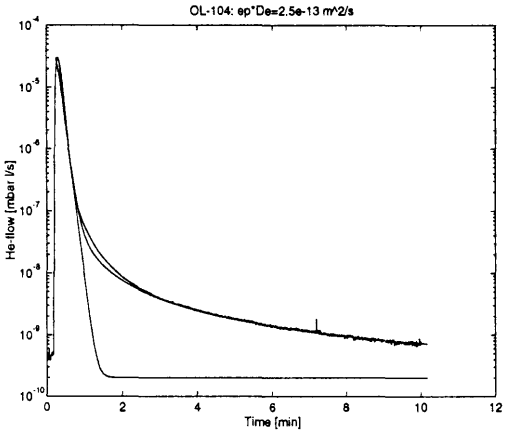

Figure 2. *Measured and fitted break-through curves for channel flow measurement on sample OL-104.*

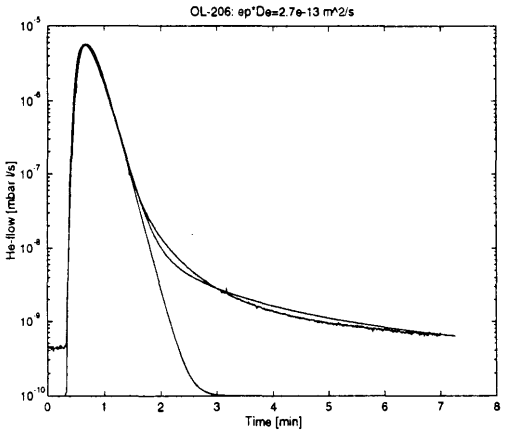

Figure 3. *Measured and fitted break-through curves for channel flow measurement on sample OL-206.*

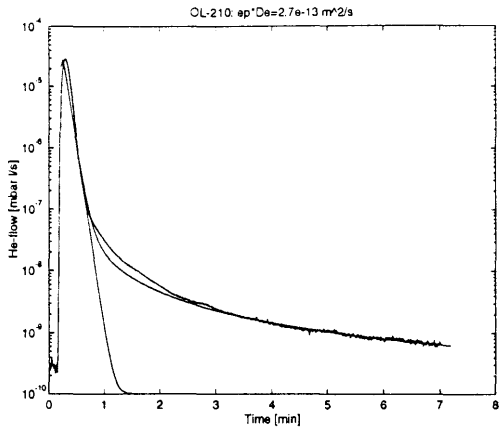

Figure 4. *Measured and fitted break-through curves for channel flow measurement on sample OL-210.*

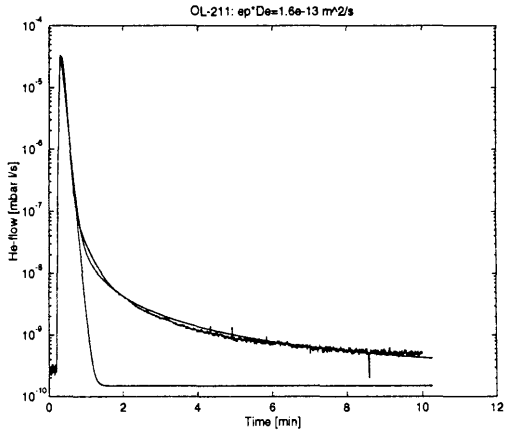

Figure 5. *Measured and fitted break-through curves for channel flow measurement on sample OL-211.*

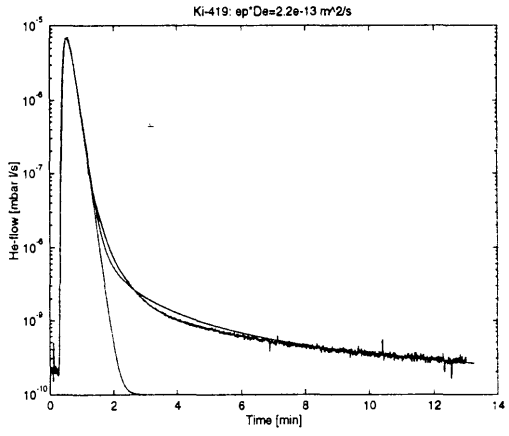

Figure 6. *Measured and fitted break-through curves for channel flow measurement on sample Ki-419.*

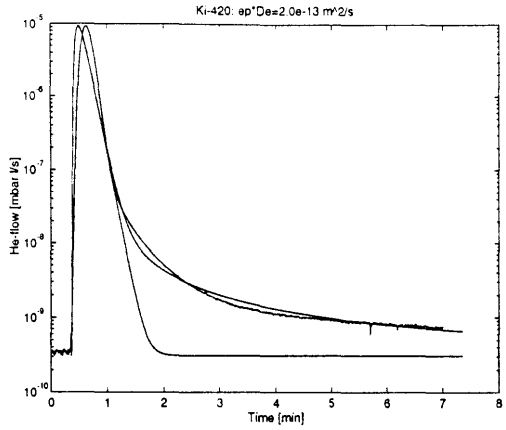

Figure 7. Measured and fitted break-through curves for channel flow measurement on sample Ki-420.

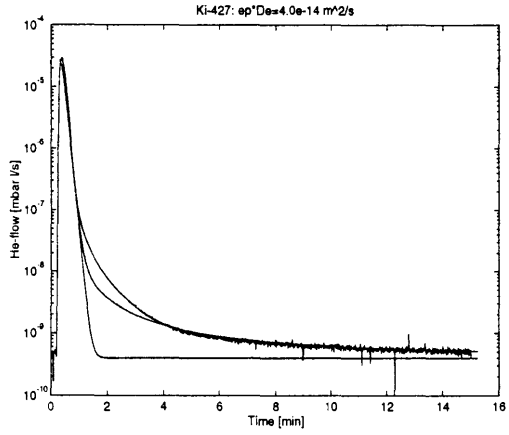

Figure 8. Measured and fitted break-through curves for channel flow measurement on sample Ki-427.

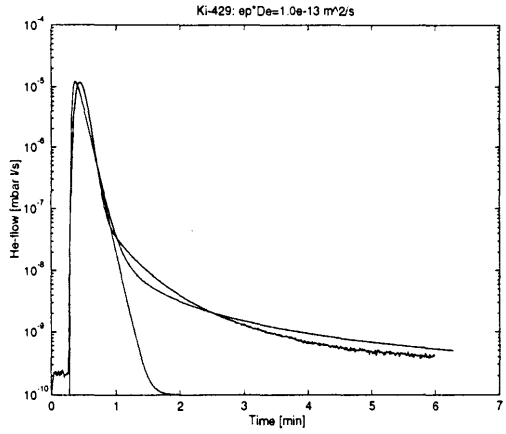

Figure 9. Measured and fitted break-through curves for channel flow measurement on sample Ki-429.

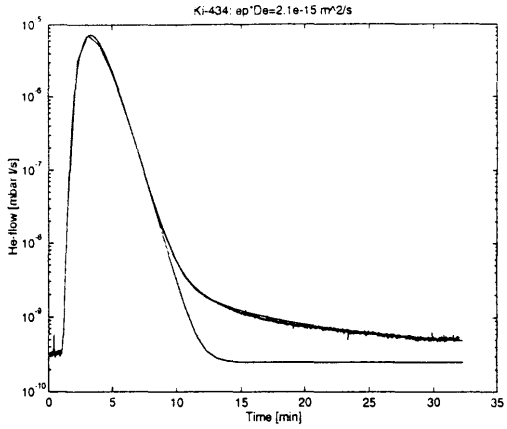

Figure 10. Measured and fitted break-through curves for channel flow measurement on sample Ki-434.

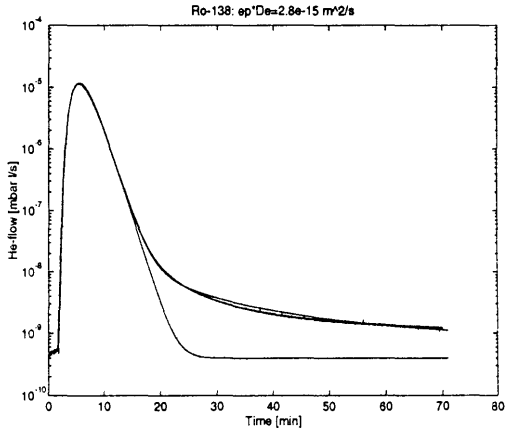

Figure 11. Measured and fitted break-through curves for channel flow measurement on sample Ro-138.

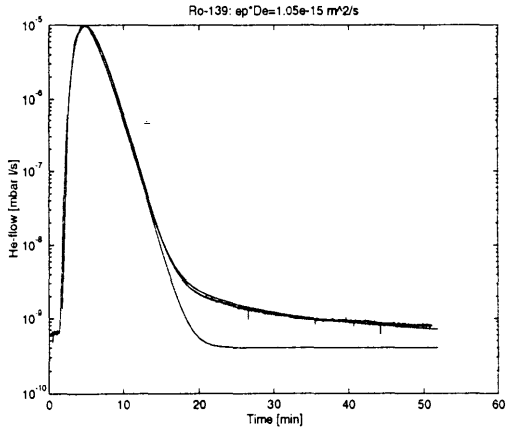

Figure 12. Measured and fitted break-through curves for channel flow measurement on sample Ro-139.

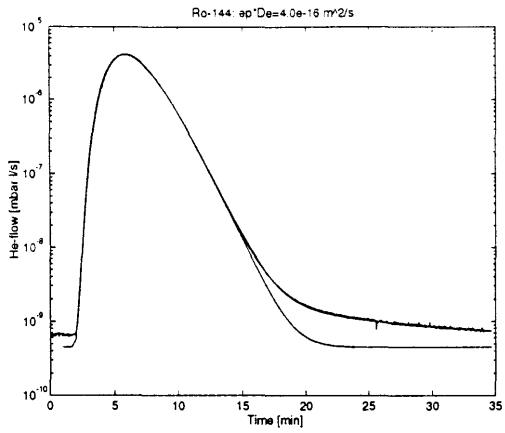

Figure 13. Measured and fitted break-through curves for channel flow measurement on sample Ro-144.

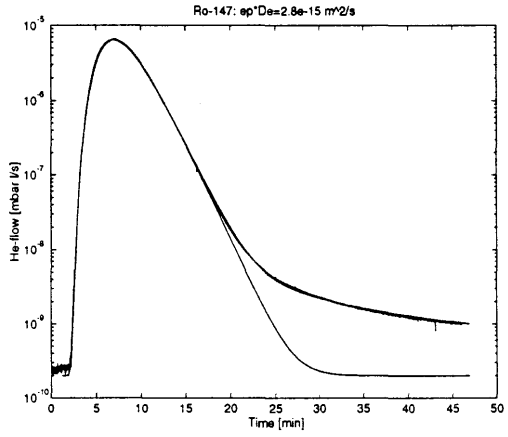

Figure 14. Measured and fitted break-through curves for channel flow measurement on sample Ro-147.

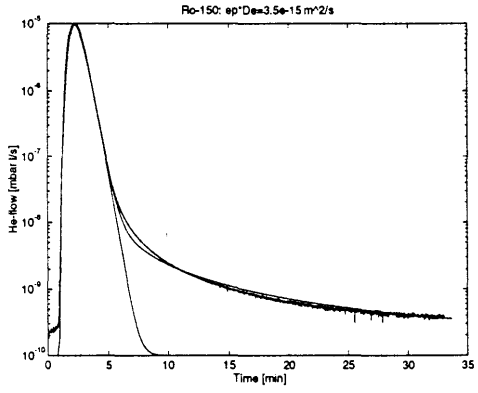

Figure 15. Measured and fitted break-through curves for channel flow measurement on sample Ro-150.

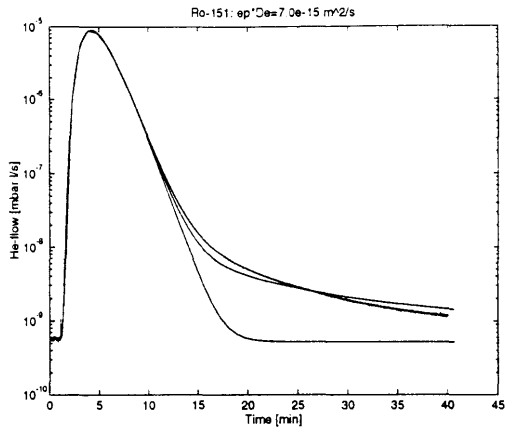

Figure 16. Measured and fitted break-through curves for channel flow measurement on sample Ro-151.

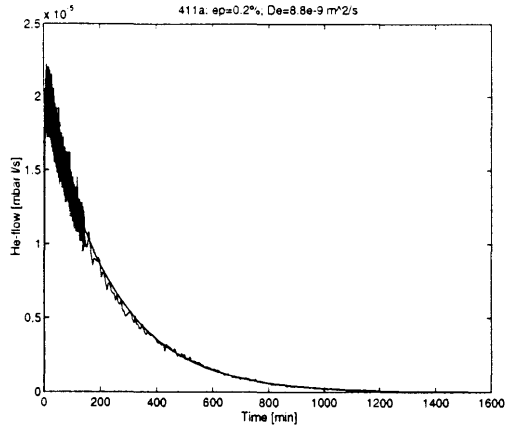

Figure 1. *Measured and fitted break-through curves for the sample Ro-1411a.*

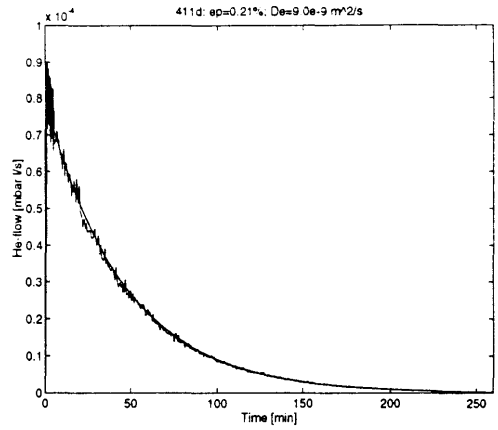

Figure 4. *Measured and fitted break-through curves for the sample Ro-1411d.*

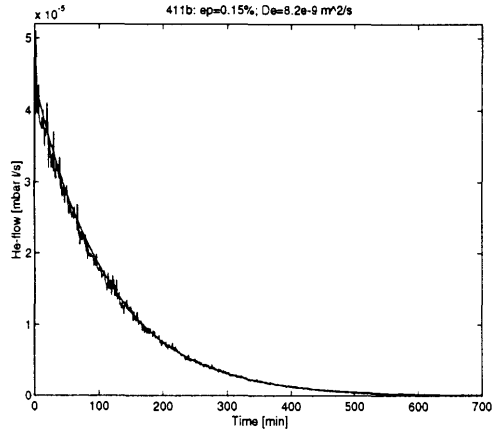

Figure 2. *Measured and fitted break-through curves for the sample Ro-1411b.*

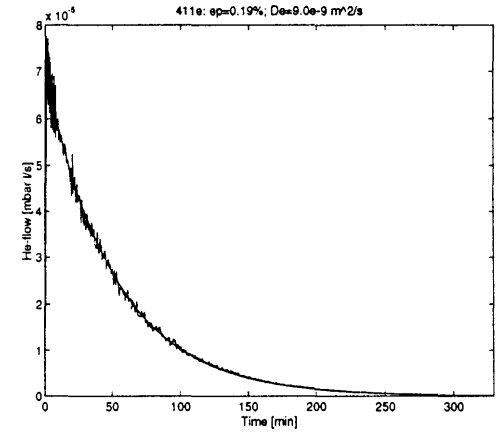

Figure 5. *Measured and fitted break-through curves for the sample Ro-1411e.*

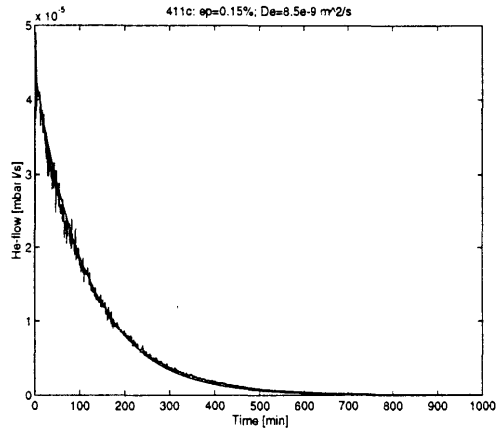

Figure 3. *Measured and fitted break-through curves for the sample Ro-1411c.*

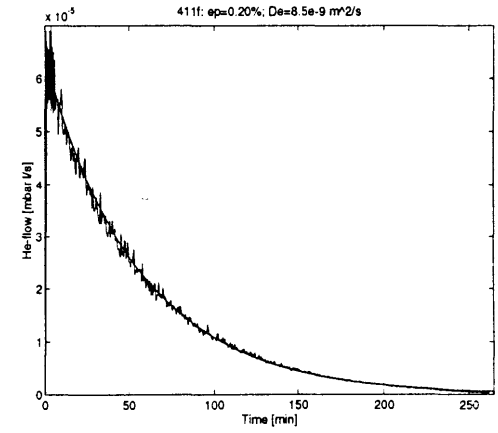

Figure 6. *Measured and fitted break-through curves for the sample Ro-1411f.*

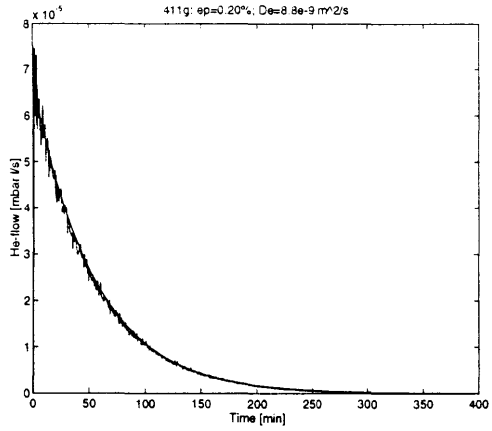

Figure 7. Measured and fitted break-through curves for the sample Ro-1411g.

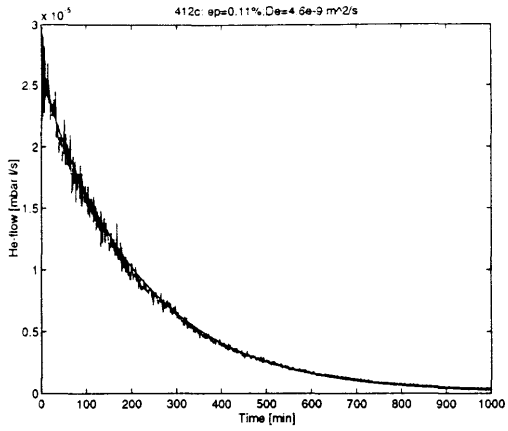

Figure 10. Measured and fitted break-through curves for the sample Ro-1412c.

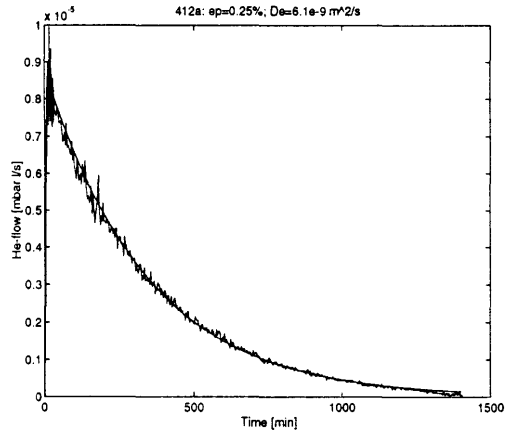

Figure 8. Measured and fitted break-through curves for the sample Ro-1412a.

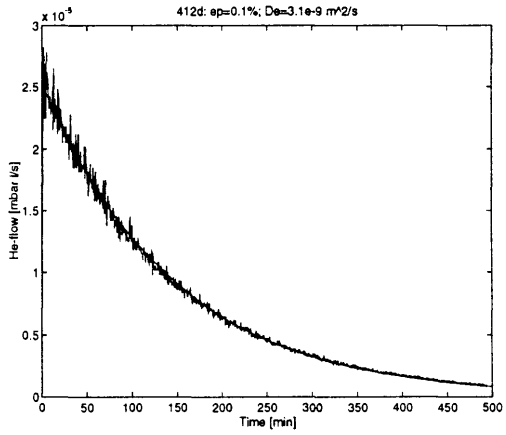

Figure 11. Measured and fitted break-through curves for the sample Ro-1412d.

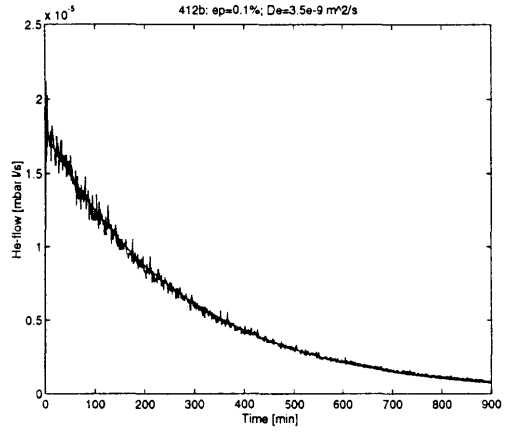

Figure 9. Measured and fitted break-through curves for the sample Ro-1412b.

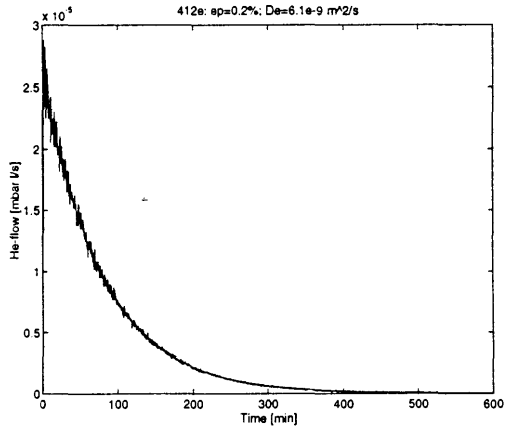

Figure 12. Measured and fitted break-through curves for the sample Ro-1412e.

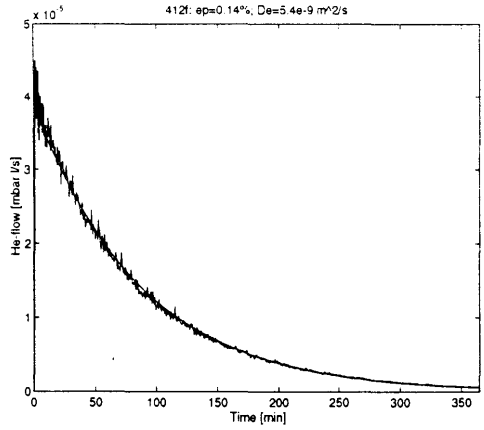

Figure 13. Measured and fitted break-through curves for the sample Ro-1412f.

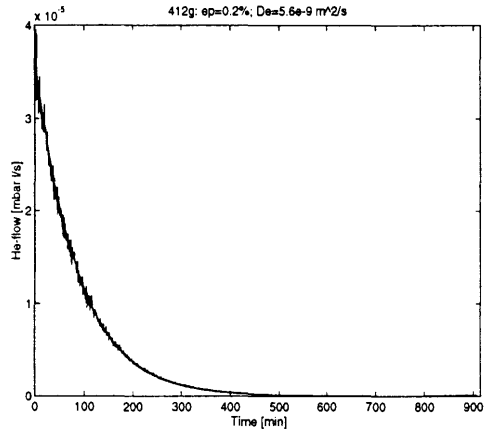

Figure 14. Measured and fitted break-through curves for the sample Ro-1412g.

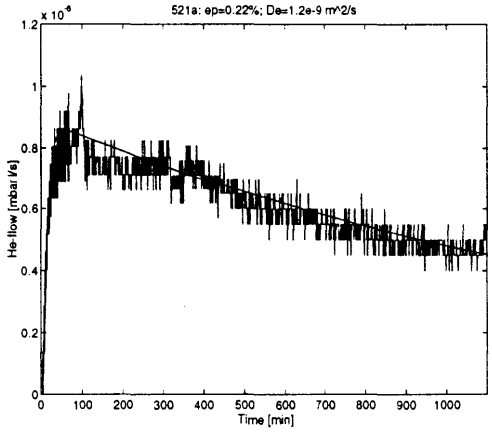

Figure 15. Measured and fitted break-through curves for the sample Ro-1521a.

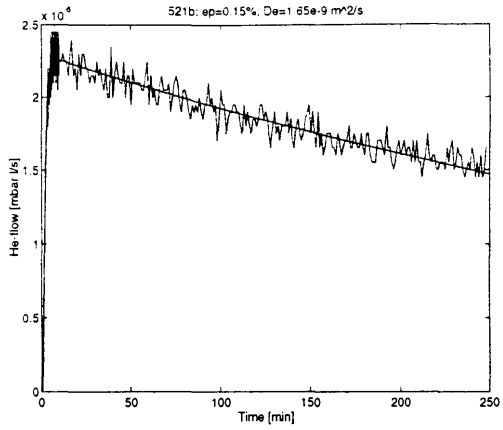

Figure 16. Measured and fitted break-through curves for the sample Ro-1521b.

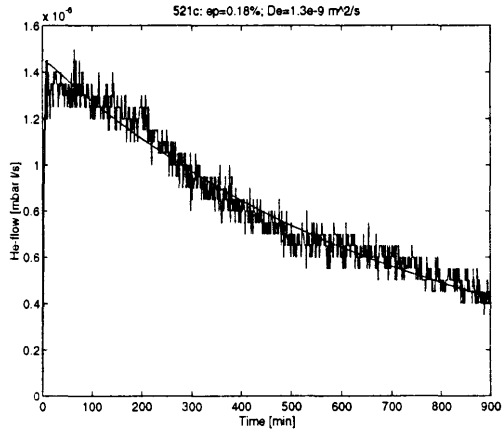

Figure 17. Measured and fitted break-through curves for the sample Ro-1521c.

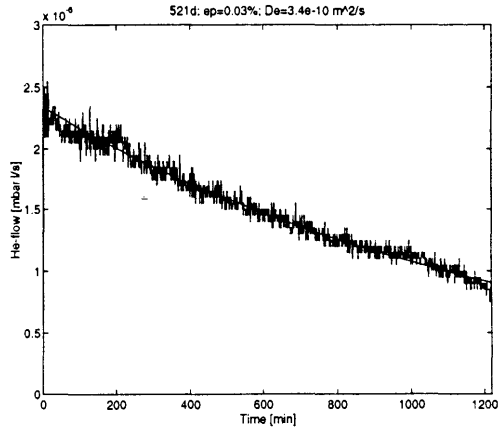

Figure 18. Measured and fitted break-through curves for the sample Ro-1521d.

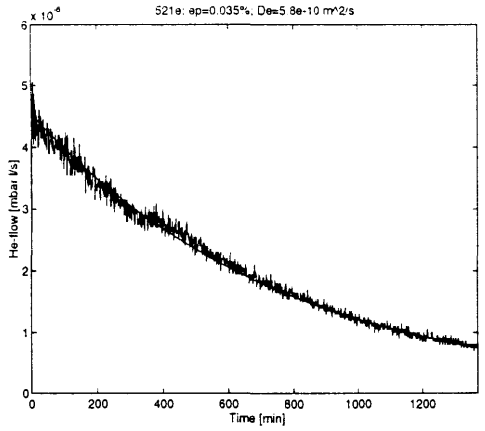

Figure 19. *Measured and fitted break-through curves for the sample Ro-1521e.*

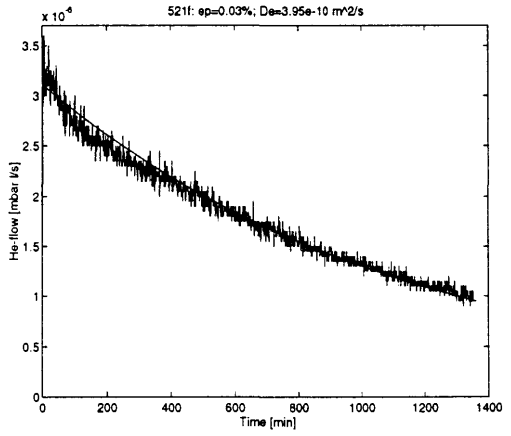

Figure 20. *Measured and fitted break-through curves for the sample Ro-1521f.*

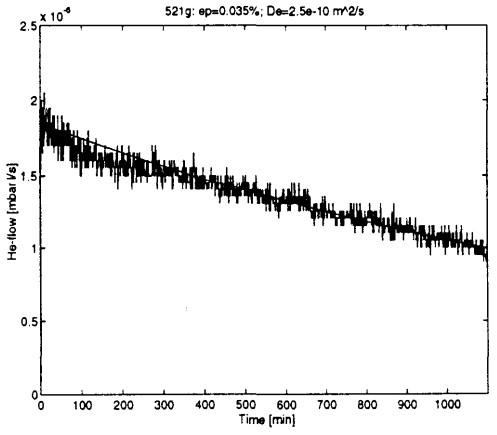

Figure 21. *Measured and fitted break-through curves for the sample Ro-1521g.*

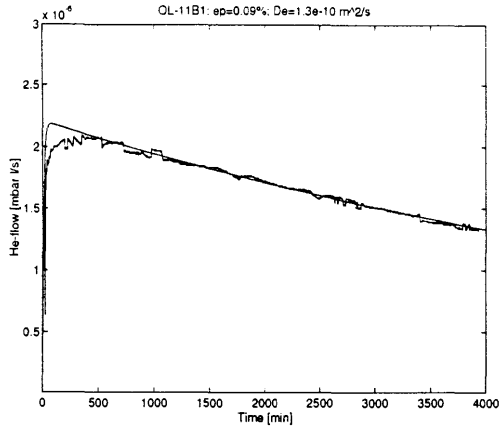

Figure 1. *Measured and fitted break-through curves for the sample OL-11B1.*

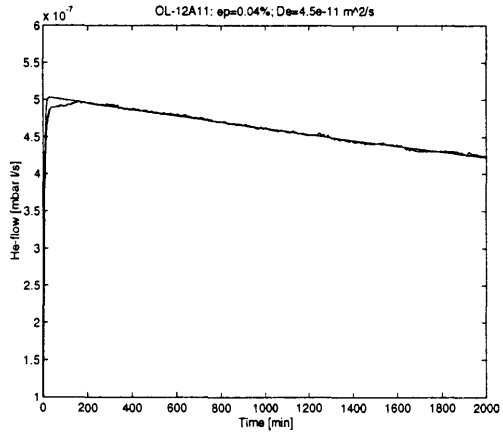

Figure 2. *Measured and fitted break-through curves for the sample OL-12A11.*

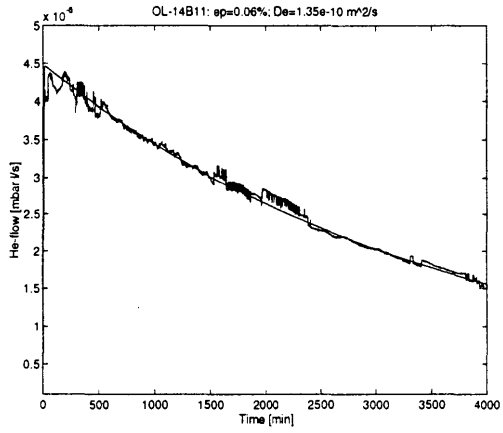

Figure 3. *Measured and fitted break-through curves for the sample OL-14B11.*

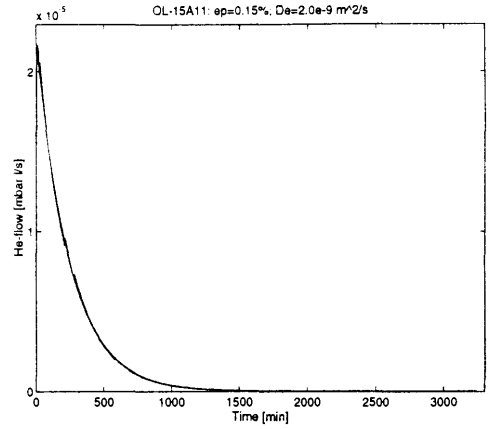

Figure 4. *Measured and fitted break-through curves for the sample OL-15A11.*

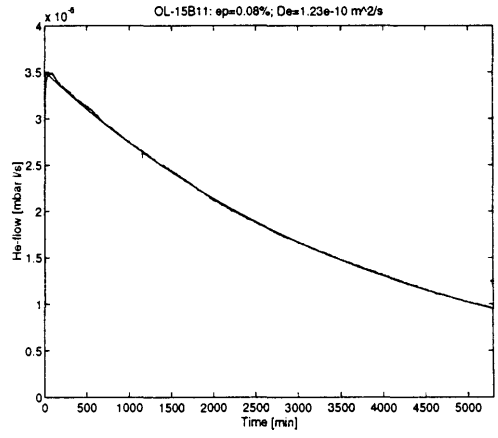

Figure 5. *Measured and fitted break-through curves for the sample OL-15B11.*

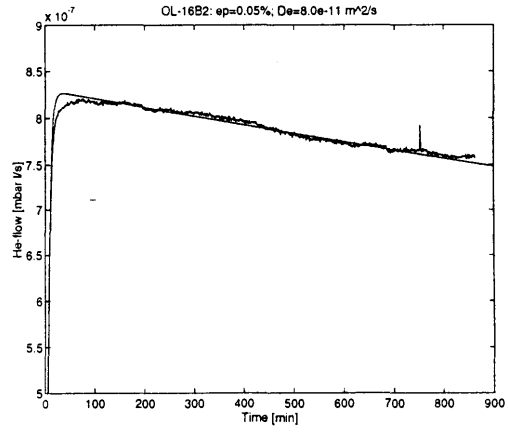

Figure 6. *Measured and fitted break-through curves for the sample OL-16B2.*

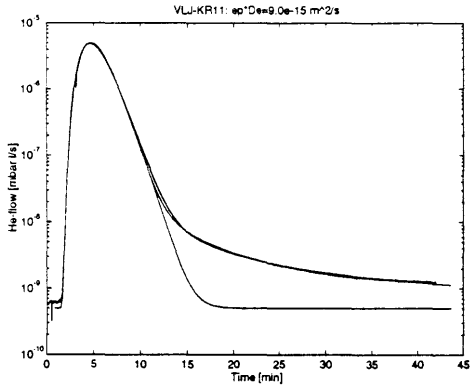

Figure 1. Measured and fitted break-through curves for channel flow measurement on sample VLJ-KR11.

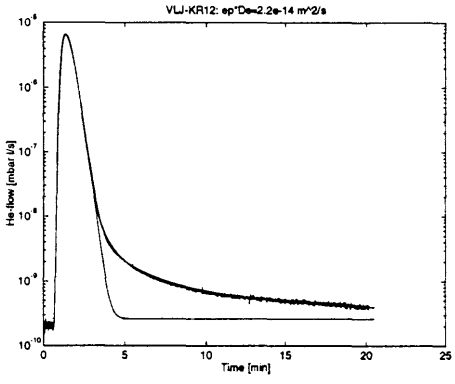

Figure 2. Measured and fitted break-through curves for channel flow measurement on sample VLJ-KR12.

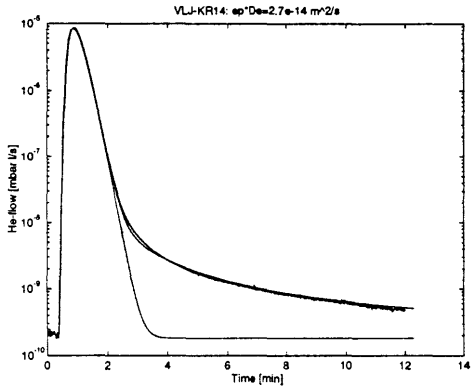

Figure 3. Measured and fitted break-through curves for channel flow measurement on sample VLJ-KR14.

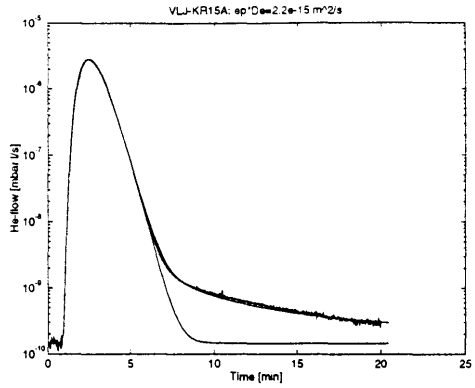

Figure 4. Measured and fitted break-through curves for channel flow measurement on sample VLJ-KR15A.

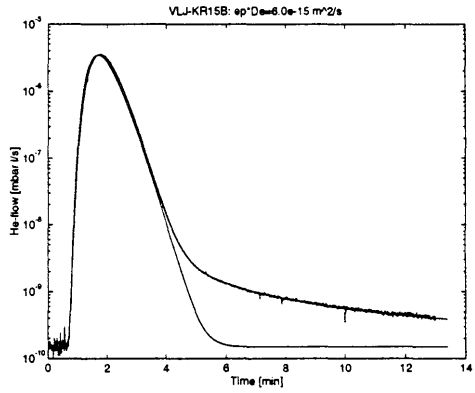

Figure 5. Measured and fitted break-through curves for channel flow measurement on sample VLJ-KR15B.

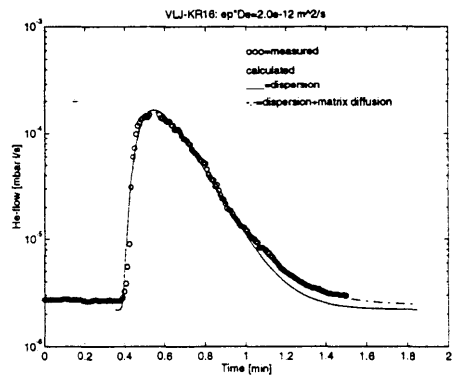

Figure 6. Measured and fitted break-through curves for channel flow measurement on sample VLJ-KR16.

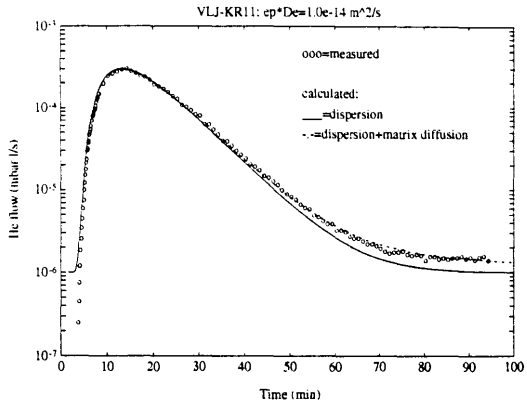

Figure 1. Measured and fitted break-through curves for in situ -measurement on hole VLJ-KR11 (depth 122-192 cm).

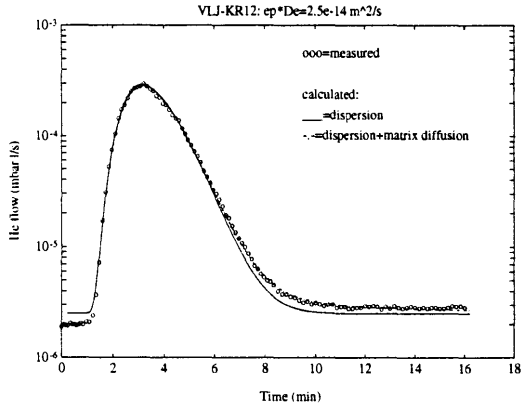

Figure 2. Measured and fitted break-through curves for in situ -measurement on hole VLJ-KR12 (depth 103-173 cm).

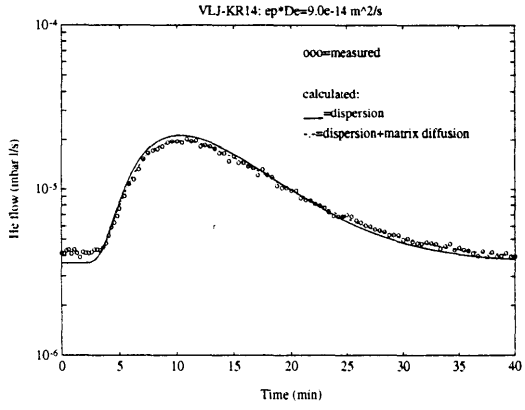

Figure 3. Measured and fitted break-through curves for in situ -measurement on hole VLJ-KR14 (depth 175-245 cm).

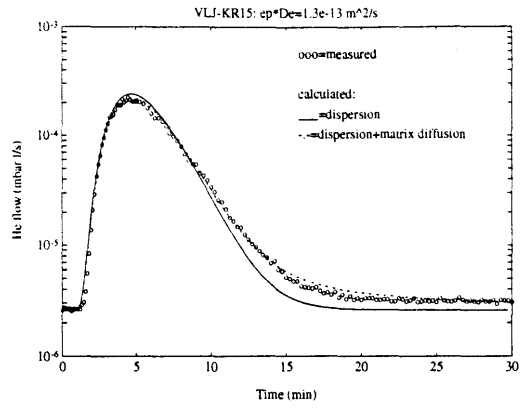

Figure 4. Measured and fitted break-through curves for in situ -measurement on hole VLJ-KR15 (depth 18-88 cm).

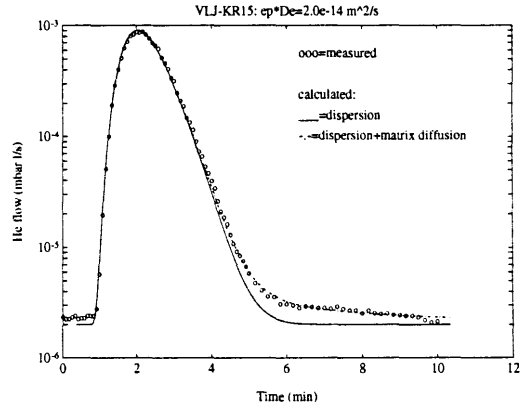

Figure 5. Measured and fitted break-through curves for in situ -measurement on hole VLJ-KR15 (depth 125-195 cm).

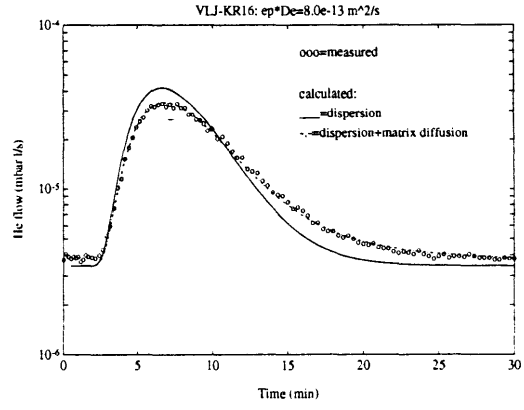

Figure 6. Measured and fitted break-through curves for in situ -measurement on hole VLJ-KR16 (depth 115-185 cm).

LIST OF POSIVA REPORTS 1997, situation 12/97

POSIVA-97-01
Model for diffusion and porewater chemistry in compacted bentonite
Theoretical basis and the solution methodology for the transport model
Jarmo Lehikoinen
VTT Chemical Technology
January 1997
ISBN 951-652-026-X

POSIVA-97-02
Model for diffusion and porewater chemistry in compacted bentonite
Experimental arrangements and preliminary results of the porewater chemistry studies
Arto Muurinen, Jarmo Lehikoinen
VTT Chemical Technology
January 1997
ISBN 951-652-027-8

POSIVA-97-03
Comparison of 3-D geological and geophysical investigation methods in boreholes KI-KR1 at Äänekoski Kivetty site and RO-KR3 at Kuhmo Romuvaara site
Katriina Labbas
Helsinki University of Technology
Material Science and Rock Engineering
January 1997
ISBN 951-652-028-6

POSIVA-97-04
Summary Report - Development of Laboratory Tests and the Stress-Strain Behaviour of Olkiluoto Mica Gneiss
Matti Hakala, Esa Heikkilä
Laboratory of Rock Engineering
Helsinki University of Technology
May 1997
ISBN 951-652-029-4

POSIVA-97-05
Radionuclide solubilities at elevated temperatures - a literature study
Torbjörn Carlsson, Ulla Vuorinen
Technical Research Centre of Finland
July 1997
ISBN 951-652-030-8

POSIVA-97-06
Surface complexation modelling: Experiments on sorption of nickel on quartz, goethite and kaolinite and preliminary tests on sorption of thorium on quartz
Esa Puukko, Martti Hakanen
University of Helsinki
Department of Chemistry
Radiochemistry laboratory
September 1997
ISBN 951-652-031-6

POSIVA-97-07

Diffusion and sorption of HTO, Np, Na and Cl in rocks and minerals of Kivetty and Olkiluoto
Vesa Kaukonen, Martti Hakanen
University of Helsinki
Department of Chemistry
Laboratory of Radiochemistry
Antero Lindberg
Geological Survey of Finland
October 1997
ISBN 951-652-032-4

POSIVA-97-08

Regression methodology in groundwater composition estimation with composition predictions for Romuvaara borehole KR10
Ari Luukkonen, Juhani Korkealaakso, Petteri Pitkänen
VTT Communities and Infrastructure
November 1997
ISBN 951-652-033-2

POSIVA 97-09

Dissolution of unirradiated UO_2 fuel in synthetic saline groundwater - Experimental methods and preliminary results
Kaija Ollila
VTT Chemical Technology
December 1997
ISBN 951-652-034-0

POSIVA 97-10

Application of surface complexation modelling: Nickel sorption on quartz, manganese oxide, kaolinite and goethite and thorium on silica
Markus Olin, Jarmo Lehikoinen
VTT Chemical Technology
December 1997
ISBN 951-652-035-9

POSIVA 97-11

FEPs and scenarios - Auditing of TVO-92 and TILA-96 against International FEP database
Timo Vieno, Henrik Nordman
VTT Energy
December 1997
ISBN 951-652-036-7

POSIVA 97-12

Principles of Mechanical Excavation
Arne Lislerud
Tamrock Corp.
December 1997
ISBN 951-652-037-5

POSIVA 97-13

Through-diffusion, permeability, channel-flow and *in situ* results for porosity and migration properties of rock samples by He-gas methods

Kari Hartikainen, Juhani Hartikainen
Oy Helium Gas Research HGR Ltd
Jussi Timonen
Department of Physics
University of Jyväskylä

December 1997
ISBN 951-652-038-3